Evidence for conservation of primordial ~12-hour ultradian gene programs in humans under free-living conditions

Bokai Zhu[1,2,3] *, Silvia Liu[2,4], Natalie L. David[1,5,6], William Dion[1], Nandini K Doshi[1,6], Lauren B. Siegel[5], Tânia Amorim[1,5,6], Rosemary E. Andrews[1,6], GV Naveen Kumar[1], Hanwen Li[7], Saad Irfan[1], Tristan Pesaresi[1,6], Ankit X. Sharma[1], Michelle Sun[1], Pouneh K. Fazeli [5,6] and Matthew L. Steinhauser [1,6,8] *

[1]Aging Institute of UPMC, University of Pittsburgh School of Medicine; Pittsburgh, Pennsylvania, USA

[2]Pittsburgh Liver Research Center, University of Pittsburgh; Pittsburgh, Pennsylvania, USA

[3]Division of Endocrinology and Metabolism, Department of Medicine, University of Pittsburgh School of Medicine; Pittsburgh, Pennsylvania, USA

[4]Department of Pathology, University of Pittsburgh School of Medicine; Pittsburgh, Pennsylvania, USA

[5]Neuroendocrinology Unit, Division of Endocrinology and Metabolism, Department of Medicine, University of Pittsburgh School of Medicine; Pittsburgh, Pennsylvania, USA

[6]Center for Human Integrative Physiology, University of Pittsburgh School of Medicine; Pittsburgh, Pennsylvania, USA

[7]Department of Statistics, Kenneth P. Dietrich School of Arts and Sciences, University of Pittsburgh; Pittsburgh, Pennsylvania, USA

[8]Division of Cardiology, Department of Medicine, University of Pittsburgh School of Medicine; Pittsburgh, Pennsylvania, USA

*Corresponding authors. Email: bzhu@pitt.edu (BZ); msteinhauser@pitt.edu (MLS)

Address:

100 Technology Drive

Bridgeside Point 1

Pittsburgh PA, 15219

Abstract:

While circadian rhythms are entrained to the once daily light-dark cycle of the sun, many marine organisms exhibit ~12h ultradian rhythms corresponding to the twice daily movement of the tides. Although human ancestors emerged from circatidal environment millions of years ago, direct evidence of ~12h ultradian rhythms in humans is lacking. Here, we performed prospective, temporal transcriptome profiling of peripheral white blood cells and identified robust ~12h transcriptional rhythms from three healthy participants. Pathway analysis implicated ~12h rhythms in RNA and protein metabolism, with strong homology to the circatidal gene programs previously identified in Cnidarian marine species. We further observed ~12h rhythms of intron retention events of genes involved in MHC class I antigen presentation, synchronized to expression of mRNA splicing genes in all three participants. Gene regulatory network inference revealed XBP1, and GABP and KLF transcription factor family members as potential transcriptional regulators of human ~12h rhythms. These results suggest that human ~12h biological rhythms have a primordial evolutionary origin with important implications for human health and disease.

52 **Introduction:**

53 Biological rhythms are conserved from single-cell organisms to humans. The relevance of
54 biological rhythms is exemplified by circadian rhythms, which are entrained to a ~24-hour cycle
55 by the rotation of the Earth and daily exposure to sunlight. Circadian gene expression programs
56 in turn regulate canonical hormonal systems, vasomotor activity, coagulation, amongst other
57 processes, accounting for predilection of certain disease events at specific times of day [1].
58 Genetic variants in core circadian genes and disruptions of circadian rhythms are associated with
59 increased risk of diverse human diseases [1-4]. The wide-ranging pathological effects of circadian
60 disruption demonstrate the centrality of the 24h circadian clock to homeostasis and disease
61 pathobiology [1].

62 Our understanding of biorhythms is expanded by alternative, non-circadian rhythms in
63 lower organisms. Coastal marine organisms, such as the sea anemone *A. diaphana,* exhibit ~12h
64 ultradian rhythms, entrained by the twice daily movements of the tides [5]. In mice, many ~12h
65 rhythms of gene expression involved in mRNA, protein and lipid metabolism are established by
66 an XBP1-dependent oscillator independent of the circadian clock or cell cycle [6, 7]. Oscillation of
67 some physiological metrics at an approximate ~12h interval in humans suggests the possibility of
68 a corresponding 12h molecular oscillator [6]. However, direct evidence for ~12h rhythms at the
69 molecular level in humans is lacking. In a recent single time-point examination of postmortem
70 human brain tissues using time-of-death as surrogate for circadian time, we uncovered ~12h
71 ultradian rhythms of gene expression in dorsolateral prefrontal cortex regions that are implicated
72 in unfolded protein response (UPR) and mitochondria-related metabolism like oxidative
73 phosphorylation [8]. While this study provided support for the existence of ~12h rhythms in
74 humans, time-of-death may not accurately reflect internal circadian time. To overcome this
75 limitation, we performed a prospective longitudinal study of three healthy participants admitted to
76 an inpatient clinical research unit for high temporal resolution (q2h) sampling of peripheral white

77 blood cells. We discovered a shared ~12h gene program with homology to our ancient marine
78 ancestors and involving fundamental pathways of protein and RNA metabolism.

79

80 **Results:**

81 **Gene expression oscillations in human white blood cells under free-living conditions**

82 We studied 3 healthy males (**Table 1**) who self-reported a regular nighttime sleep
83 schedule and did not engage in nighttime shift work or other sleep-disrupting activities and who
84 had a body mass index between 18.5-24.9 kg/m^2. Participants were admitted for a 1-day
85 acclimatization period prior to 48 hours of blood sampling at a 2-hour sampling interval (**Fig. 1A**),
86 a frequency that allowed detection of oscillations with periods of 6 hours or longer with high
87 confidence [9, 10]. The protocol reflected our aim to sample with sufficient frequency and duration
88 to detect ~12h rhythms within individuals. We also sought to mimic free-living conditions by
89 feeding them a diet similar in caloric content and macronutrient composition to their typical intake
90 and encouraging maintenance of their routine sleep/wake cycles. Overnight, blood was collected
91 via a long intravenous line from outside the room to avoid exposing participants to light or sleep
92 disruption.

93 We performed bulk mRNA-Seq in buffy coat fractions prospectively collected at 2h
94 intervals for 48 hours (24 samples/participant) (**Fig. 1A**) (**Table S1**). To identify genes cycling with
95 a period ranging from 6 to 32 hours, we applied the RAIN algorithm to each individual's temporal
96 transcriptome [11]. Compared to other competing methods like JTK_CYCLE, RAIN detects
97 rhythms with arbitrary waveforms and therefore more robustly uncovers ultradian rhythms [10, 12,
98 13]. As shown in **Fig. 1B**, we observed inter-individual variability in the number of genes cycling
99 at different periods. Specifically, the first individual exhibited dominant oscillations cycling at the
100 circadian period between 20-24 hours, with a secondary population detected at the periods of 10-

101 12 hours. These 10-12h oscillations were more evident in the first 24 hours, with dampening of
102 ultradian rhythms on the second day (**Fig. 1B**). Aside from circadian oscillations between 18 and
103 24 hours, the second participant exhibited ultradian rhythms cycling at periods of 6 and 12-hours
104 (**Fig. 1B**). The third individual also exhibited oscillations cycling at 6-hours, 12-hours, and at ~20
105 hours, with very few genes observed cycling at 24-hours (**Fig. 1B**). The inter-individual variability
106 of the oscillating transcriptome profiles in our study may be attributable to the fact that the
107 participants were held at living conditions that resemble free-living. By contrast, in a prior study
108 that prospectively examined circadian gene expression in human white blood cells, participates
109 were maintained in a semi-recumbent position under dim light and constant temperature and
110 humidity during 40 hours of sleep deprivation [14].

111 To increase statistical power to detect oscillations common to all three individuals, we
112 performed a meta-analysis and generated a combined p-value for each gene at periods from 6-
113 to 32-hours using Fisher's method. This method has been extensively used in medical and genetic
114 research to combine the results from independent tests with the same null hypothesis [15]. In our
115 case, each participant was distinct and studied at a different time, however the null hypothesis
116 was the same: the absence of rhythms. Using combined p-values (herein referred to as meta p
117 values) with an alpha of 0.05, we observed two major populations of oscillations cycling at 12-
118 and 18-24-hours, with the largest number of genes observed cycling at 20-hours (**Fig. 1B**). Using
119 the Benjamini-Hochberg procedure to further adjust for the false discovery rate on meta p values
120 (meta adj-P value or FDR), we uncovered 653 circasemidian (~12h) and 5,453 circadian (~24h)
121 genes with an FDR less than 0.05 (**Fig. 1C**) (**Table S2**).

122

123 **Human white blood cells exhibit rhythmicity in canonical circadian genes.**

124 To determine the soundness of our RNA-seq dataset, we compared our putative circadian
125 gene set to a prior study, where participants were maintained in much more stringently controlled

126 conditions of dim-lighting, fixed semi-recumbent positioning, and sleep deprivation [14]. In that
127 study, a total of thirteen circadian genes exhibiting robust circadian expression in peripheral white
128 blood cells were utilized as a training gene set to predict the circadian phases from single time
129 point blood samples [14], of which seven and nine exhibited meta adj-P values less than 0.05 and
130 0.1, respectively, in our study (**Fig. 1D**). This set includes canonical circadian clock genes *PER1*,
131 *PER2*, *PER3*, *NR1D1*, *NR1D2* and *CRY1* (**Fig. 1D, E**). Gene set enrichment analysis (GSEA)
132 further indicated that the forty circadian genes that cycled in at least 50% of the human
133 participants in that study also exhibited circadian oscillations with low meta p values in our study
134 (**Fig. 1F**). For these core circadian genes we observed inter-individual variability in the phases
135 and amplitudes among the three participants (**Fig. 1E**), likely reflecting individual-specific sleep-
136 wake schedules. Interestingly, even under constant routine conditions, these genes also exhibited
137 inter-individual variability in phase and amplitudes, albeit to a much less degree (**Fig. S1**). Overall,
138 circadian genes in human peripheral white blood cells are strongly involved in pathways of platelet
139 activation, regulation of actin cytoskeleton and adhesions (**Fig. 1G**). Collectively, these results
140 demonstrated the robustness of our study design and dataset, further justifying the treatment of
141 each longitudinal time series as an independent dataset followed by a meta-analysis to achieve
142 greater statistical power.

143

144 **~12h ultradian rhythms of gene expression are involved in mRNA and protein metabolism**
145 **in human peripheral white blood cells.**

146 Oscillations cycling close to a 12-hour period were the second most abundant in all three
147 individuals after the circadian population (**Fig. 1B**). Using meta adj-P values (FDR) as cut-off, we
148 identified 653 and 2,768 ~12h genes (with period between 10-14-hours) with meta adj-P (FDR)
149 less than 0.05 and 0.1, respectively (**Figs. 1C and 2A**). Importantly, the average gene expression

150 profiles of these 653 (FDR<0.05) and 2,115 (0.05<FDR<0.1) genes are very similar to each other
151 in each of the three individuals (**Fig. 2A**).

152 As observed with circadian genes, inter-individual variability was also observed for ~12h
153 ultradian rhythms. In the first and second participants, the acrophases (time of gene expression
154 peak) were at 8 am and 8 pm, while ~12h rhythms in the third individual peaking around 4 am
155 and 4 pm (**Fig. 2A**). Examples of robust ~12h genes cycling in all three individuals include *MYDGF*,
156 *ICMT*, *RNF7*, *TCEB1*, *MFF* and *OXA1L* (**Fig. 2B**). *MYDGF* encodes an endoplasmic reticulum
157 (ER)-localized protein with secreted forms also identified from monocytes/macrophages that
158 promotes tissue repair in a murine model of myocardial infarction [16, 17]. *ICMT* encodes a
159 protein-*S*-isoprenylcysteine *O*-methyltransferase that also localizes in the ER and is responsible
160 for cell membrane-targeting of selective proteins [18]. *RNF7* encodes an essential subunit of
161 SKP1-cullin/CDC53-F box protein ubiquitin ligases [19] and TCEB1 protein is a subunit of the
162 transcription factor B responsible for transcription elongation [20]. Both MFF and OXA1L are
163 mitochondrial proteins localized to outer and inner mitochondria membranes, respectively, and
164 are essential for mitochondria fission and assembly of respiratory complex I [21, 22].

165 One important question regarding ultradian rhythmicity is whether it reflects 'real' rhythms
166 with biological significance, or simply mathematical artefact. This is particularly relevant for
167 rhythms that cycle at harmonic frequencies of the 24-hour circadian period, as non-sinusoidal
168 circadian waveforms (seesaw-like or square-shaped waveforms) often have superimposed ~12
169 and ~8-hour harmonic frequencies detected by spectral analytical methods such as a Fourier
170 transformation, eigenvalue/pencil, or wavelet analyses [12, 23-25]. We took several approaches
171 to address this question. First, 12-hour transcriptional oscillations did not cycle at the exact
172 second harmonic of the dominant circadian period in any of the three participates: the first
173 harmonic circadian periods were 22, 18 and 20-hours in the three individuals, respectively, and
174 20-hours for the meta-analysis (**Fig. 1B**). Second, if ~12h oscillations are indeed harmonics of

175 the circadian rhythm, then genes exhibiting both circadian and ~12h ultradian rhythmicity should
176 be detected at a higher frequency than expected by chance. To test this, we generated a circadian
177 gene set using a 4-hour interval subset of the original dataset (8am, 12am, 4pm, etc.) to achieve
178 an equivalent number of data points per period—i.e. equivalent sensitivity—and a meta-p cut-off
179 of 0.05. Importantly, the circadian subset showed a strong positive correlation with meta-p values
180 obtained with the full 2h interval dataset (**Fig. S2A**). After this adjustment to match sampling
181 interval to period ratios, ~12h gene rhythms were more prevalent than circadian genes (**Fig. 2C**).
182 Moreover, the expected and observed percentages of genes having circadian and/or ~12h
183 rhythms were nearly identical (p=0.73 by Chi-square test), indicating independent detection of
184 ~12h and circadian rhythms (**Fig. 2D**). Third, we performed Gene Ontology (GO) and GSEA to
185 compare biological pathways enriched in circadian and ~12h genes, respectively. We reasoned
186 that if ~12h oscillations are mathematical harmonics of the circadian rhythm, then ~12h and
187 circadian genes should share enriched biological pathways. Both analyses revealed largely
188 distinct pathways associated with circadian and ~12h rhythms (**Figs. 2E and S2B**). While
189 circadian rhythms were enriched in platelet activation, blood coagulation and cell adhesion as
190 previously demonstrated (**Figs. 2E and S2B**), ~12h genes were associated with fundamental
191 biological processes of mRNA (such as spliceosome and RNA splicing), protein metabolism
192 (including ubiquitin-mediated proteolysis, response to ER stress, protein folding and protein
193 transport in the ER and Golgi), and mitochondria complex chain assembly (**Figs. 2E and S2B**).
194 Cytoplasmic translation, on the other hand, was enriched in both circadian and ~12h genes (**Fig.
195 S2B**). Consistent with the known causal roles of dysregulated proteostasis in proteinopathies,
196 and impaired mitochondrial metabolism in metabolic syndromes, ~12h genes were also much
197 more strongly enriched in neurogenerative disease gene sets and nonalcoholic fatty liver disease
198 (**Fig. 2F**). Enrichment of protein metabolism and mitochondrial respiration genes is also in
199 alignment with ~12h gene signatures in human dorsolateral prefrontal cortex [8].

200 We next performed pathway analyses of the ~12h gene sets for each individual participant.
201 We either analyzed the data as a continuous 48h time series with a single data point at each time
202 point (RAIN conti) or as a 24h time series where data points collected at the same time on two
203 consecutive days were treated as biological replicates (RAIN dupli) (**Table S2**). The RAIN
204 duplicate approach revealed larger ~12h gene programs (p value cut-off of 0.05) with lower FDRs:
205 3,462 genes (FDR=0.224), 7,060 genes (FDR=0.119) and 4,807 genes (FDR=0.166) (**Figs. S3**
206 **and 4**). As expected, ~12h genes common to all three individuals also tended to have small meta-
207 p values (**Fig. S3E and Fig. S4E**). Pathways related to mRNA and protein metabolism emerged
208 as significantly enriched for 12h rhythm genes in each participant regardless of the inputs or
209 thresholds for RAIN analysis (**Figs. S3G and S4C, E**).

210 To determine robustness to different analytic methods, we also performed spectrum
211 analysis with the eigenvalue/pencil method [10, 12, 13, 26-28], which unlike statistical methods
212 such as JTK_CYCLE and RAIN does not require pre-assignment of period range and thus allows
213 unbiased identification of multiple oscillations for any given gene [10, 12, 13, 26-28].
214 Eigenvalue/pencil analyses also revealed prevalent circadian and ~12h oscillations in all three
215 individuals (**Figs. S5-7**, **and Table S3**). Since the eigenvalue/pencil algorithm involves non-
216 statistical signal processing, we used a permutation-based method that randomly shuffles the
217 time label of gene expression data to determine the false discovery rate (FDR) for the 12h gene
218 list [13, 29]. The FDR for the ~12h gene lists was estimated to be 0.33, 0.36 and 0.38 for each of
219 the three participants respectively (**Figs. S5F, S6F, and S7F)**. It is important to note that the
220 calculated FDR is likely an overestimation since amplitude and phase information for the ~12h
221 rhythms is not considered. Application of eigenvalue/pencil analyses confirmed that 1) ~12h gene
222 expression was dampened in the second day in the first individual but remained steady over 48
223 hours in the second and third participants (**Figs. S5G, S6G, and S7G**), 2) ~12h rhythms peaked
224 around 8am and 8pm in the first and second individuals, and around 4am and 4pm in the third

225 (**Figs. S5C, S6C and S7C**), and 3) ~12h genes were strongly enriched in mRNA and protein
226 metabolism pathways and distinct from the circadian gene sets in all three individuals, (**Figs. S5J,**
227 **S6J and S7J**). In addition, we found that the relative amplitude (amplitude normalized to the mean
228 expression of each gene) of ~12h rhythms in all three individuals are less than their respective
229 circadian counterparts, with mean fold change of 2.74, 1.88 and 1.67 observed in the three
230 individuals (**Figs S5E, S6E, and S7E)**. The smaller relative amplitude of ultradian compared to
231 circadian gene expression rhythms has been also observed in mice [12], and may be due to
232 physical restraints on the maximal rates of RNA polymerase II-mediated transcription can achieve
233 [12]. Taken together, multiple analytical methods and statistical thresholds provided convergent
234 evidence supporting the existence of ~12h rhythms of gene expression implicated in mRNA and
235 protein metabolism in human white blood cells.
236
237 **Identification of candidate transcriptional regulators of ~12h rhythms**
238 To infer gene regulatory networks governing ~12h rhythms in human white blood cells, we
239 performed LISA [30] and motif analysis on the top 500 ~12h genes with the lowest meta-p values.
240 We cross-referenced enriched motifs with transcription factor genes that exhibited ~12h rhythms
241 (with meta-adjP<0.1), identifying XBP1, CREBZF, GABPB1/2, NFYB, GMEB1, KLF16 as top
242 candidates that are preferentially enriched with ~12h genes compared to circadian genes (**Fig.**
243 **3A-D**). XBP1, CREBZF and CREB1 belong to the Basic Leucine Zipper (bZIP) transcription factor
244 family and are established transcription regulators of the UPR and adaptive stress response [31-
245 35]. GABPB1/B2 are ETS family transcription factors involved in mitochondria biogenesis and
246 oxidative phosphorylation [36, 37]. NFYB encodes one of the three subunits of nuclear
247 transcription factor Y (the other being NFYA and NFYC) and its DNA binding motif was recently
248 shown to co-occur with XBP1 in mouse type-2 T helper cells [38]. Importantly, that many of these
249 transcription factors have been implicated in regulation of ~12h rhythms in mice. For instance, it
250 was previously proposed that ~12h rhythms are generally established by a tripartite network

251 comprising ETS, bZIP and NFY transcription factors, whereas KLF transcription factors may
252 control ~12h rhythms in a more tissue specific manner [39]. Enriched GMEB DNA binding motifs
253 were also observed in the promoters of hepatic ~12h rhythms in mice [26].

254 We next incorporated a recently published XBP1 ChIPmentation dataset from mouse T
255 helper cells into our analysis [40]. We found that XBP1 target genes—those genes directly bound
256 by XBP1 and whose expression is reduced in the absence of XBP1—were significantly enriched
257 in the putative ~12h human gene set, but not in the circadian gene set (**Fig. S8A-C**). This included
258 the mRNA processing genes *Tceb1*, *Thoc6*, *Smu1*, *Snrnp53*, *Eny2* and *Snrpc*, mitochondria
259 metabolism-related genes such as *Gabpa*, *Mrpl40* and *Mrpl27,* and proteostasis genes *Mydgf*,
260 *Rnf7*, *Serp1* as well as *Xbp1* itself (**Fig. S8A**). These results suggest XBP1, GABP and KLF
261 transcription factor family members as candidate transcriptional regulators of ~12h rhythms in
262 human white blood cells, with XBP1 a strong candidate given its previously identified role as a
263 major regulator of 12h transcriptional oscillations in the murine liver [13].
264

265 **~12h rhythms are synchronized to RNA splicing functionality.**

266 Given representation of RNA metabolism and mRNA splicing pathways in ~12h
267 transcriptional rhythms, we tested whether such oscillations would translate into a downstream
268 functional effect in the form of alterations in mRNA splicing. We interrogated the RNA-seq data
269 for evidence of rhythmicity in intron retention (IR) events, predicting that if the rhythm of RNA
270 splicing genes' transcription was functionally relevant, it would temporally correlate with global IR.
271 We applied a recently published algorithm iREAD [41]. Using two different criteria for defining
272 retained introns, we identified ~12h rhythms of global IR events in all three participants (with meta-
273 $p<0.003$) (**Figs. 3E, F and S9A-D**). IR rhythms were synchronized to the expression of mRNA
274 splicing genes (**Figs. 3E, F and S9A-D**). These data suggest synchronization of mRNA splicing

275 gene programs to splicing functionality, further implicating 12h rhythms in the regulation of RNA
276 metabolism.

277 We next performed GO analysis on the set of transcripts in which we detected retained
278 introns. While the GO terms associated with intron retention genes were largely consistent at the
279 morning and evening peaks, we also observed differential enrichment in a subset. The morning
280 intron retention gene sets were enriched in immune functions, especially those involving the
281 display of intracellular peptide fragments to cytotoxic T cells via MHC class 1 complexes (*e.g.,*
282 HLA-A/C/E and B2M), whereas the evening intron retention gene sets exhibited greater
283 heterogeneity across the three participants (**Figs. S10, 11**). Taken together, these data suggest
284 that one function of human ~12h rhythms in peripheral leukocytes might be the anticipatory
285 splicing of antigen presentation genes.
286

287 **Evolutionary conservation of ~12h gene programs and function**

288 ~12h rhythms in coastal and estuarine animals suggest an ancient evolutionary origin [6,
289 39, 42-46] (**Fig. 4A**). To test for homology between the hitherto identified human ~12h rhythm
290 genes and circatidal genes in marine animals, we compared the most robust ~12h human genes
291 (meta-adjP less than 0.10) with the circatidal gene program uncovered in *Aiptasia diaphana* [47],
292 a sea anemone species which shares a eumetazoan ancestor with *Homo sapiens* ~700 million
293 years ago in the Cryogenian period [48]. In line with our human data, the most enriched biological
294 pathways amongst *A. diaphana* circatidal genes were mRNA processing and protein metabolism,
295 distinct from those enriched in the circadian genes, which included pathways of carbohydrate
296 metabolism and detoxification [44] (**Fig. S12A**). We found 404 ~12h genes common to both
297 species, a number significantly higher than the expected value of 263 if there was no evolutionary
298 conservation (p=4.6e-23 by Chi-square test) (**Fig. 4B**). This subset was also enriched in mRNA
299 splicing and proteostasis pathways (**Fig. 4C-D**). We confirmed the evolutionary conservation of

300 ~12h rhythms of gene expression between human and *A. diaphana* by using two additional gene
301 sets of human ~12h genes: 653 gene set with meta-adjP values less than 0.05 (**Fig. 1C**), or the
302 851 gene set shared in all three individuals depicted in **Fig. S4B** (**Fig. S12B, C**). Protein
303 processing in the ER was the most consistently enriched GO term using the different selection
304 criteria for ~12h genes (**Fig. S12B, C**). In contrast to ~12h ultradian rhythms, we found modest
305 evolutionary conservation of circadian gene expression between human (with meta-adjP value
306 less than 0.10) and *A. diaphana* (p=0.049 by Chi-square test), with the 102 common circadian
307 genes moderately enriched in carbohydrate metabolism and detoxification pathways (**Fig. S12D-**
308 **F**).

309 If the 12-hour gene program is conserved from coastal invertebrates to humans, we
310 reasoned that lower mammals like mice should also exhibit oscillations in similar gene programs.
311 We re-examined a previously published temporal hepatic RNA-seq data set in mouse liver and
312 found 666 ~12h genes common to both human and mouse (p=2.02e-21 by Chi-square test), again
313 highly enriched in mRNA splicing and protein processing pathways (**Fig. 4E-G**). We identified 139
314 ~12h genes common to all three species: human, mouse, and *A. diaphana*, which exceeded the
315 97 expected by chance (p=1.41e-7 by Chi-square test) (**Fig. 4H**). These 139 genes are enriched
316 in protein processing in ER, spliceosome, and nucleocytoplasmic transport, the three pivotal steps
317 in central dogma information flow. Specific examples include DNAJA1, a heat shock protein 70
318 cochaperones [49], UGGT1 that serves as the predominant ER glycoprotein quality control sensor
319 [50] and *EIF2S1*, encoding the alpha subunit of the translation initiation factor eIF2 protein
320 complex [51] (**Fig. 4I-J**). These results are congruent with our previous work in murine liver in
321 identifying a regulatory function for ~12h oscillator in central dogma information flow [13].

322 Finally, we tested for synchronization between the ~12h rhythms and RNA splicing in mice
323 by performing intron retention analysis of our previously published temporal RNA-seq data from
324 mouse liver [13]. Similar to the human data, we observed strong alignment between ~12h rhythms

325 in splicing gene expression and global intron retention events peaking at the two 'rush hours' (CT2
326 and CT14) (**Fig. 4K**). In addition, liver-specific genetic ablation of XBP1 (the transcriptional
327 regulator of murine hepatic 12h oscillations) abolished ~12h rhythms of splicing gene expression
328 and intron retention rhythms, leading to constant intron retention across the day (**Fig. 4K**). These
329 collective data support evolutionary conservation of a ~12h gene program in humans related to
330 RNA and protein metabolism.
331
332 **Discussion:**
333 In this study, we discovered a ~12h regulatory network in healthy humans, controlling
334 gene programs related to fundamental processes of mRNA and protein metabolism. Remarkably,
335 conservation of ~12h rhythms in humans extended to specific gene orthologs and functional
336 pathways present in marine animals. Our discovery of one such 12h pathway, 'mRNA splicing,'
337 provided an opportunity to establish functional significance through identification of corresponding
338 12h rhythms in global intron retention events. Moreover, pathway analyses of rhythmic intron
339 retention suggests that one functional consequence of 12h rhythms in human white blood cells
340 could be rhythmic antigen presentation by splicing of MHC class I gene transcripts. We further
341 demonstrate conservation of a potential major 12h transcriptional regulator, *XBP1,* which
342 regulates 12h gene oscillations in mice [13]. *XBP1* not only exhibited 12h rhythmicity in our human
343 participants but was also implicated by gene regulatory network inferences as a lead candidate
344 regulator of human 12h gene programs. What adaptive advantage might 12h rhythms of gene
345 expression confer? We reason that the ancient ~12h rhythms that evolved in marine species in
346 response to tidal cues have been coopted by humans as an adaptive response to accommodate
347 physiological transitions related to feeding, physical activity, and sleep that are temporally
348 concentrated at dawn and dusk.

349 While our study provides evidence of 12h rhythms of gene expression in humans inclusive
350 of potential transcriptional regulators, it does not establish causality, nor does it fully address their
351 relationship with the circadian clock. At least three mutually non-exclusive mechanisms have been
352 proposed to explain the origin and regulatory mechanisms of ~12h rhythms in mice, namely that
353 they are not cell-autonomous and controlled by a combination of the circadian clock and
354 environmental cues [25, 52, 53], that they are regulated by two anti-phase circadian transcriptional
355 factors in a cell-autonomous manner [54], or that they are established by a cell-autonomous ~12-
356 hour oscillator [12, 13, 26, 28, 55, 56]. Future studies will be required to test whether candidate
357 12h regulatory factors are causal drivers of 12h gene expression rhythms and any direct
358 relationship with the circadian clock. Such mechanistic studies are challenging in humans
359 because prospective genetic manipulations cannot be performed. However, several potential
360 future directions hold promise to advance a mechanistic basis for 12h rhythms, including
361 longitudinal profiling of DNA binding by putative 12h transcriptional regulators at genome scale,
362 temporal transcriptomic/cistromic profiling of human cohorts that exhibit genetic variation in
363 candidate 12h regulatory factors, and assessment of the modifying effects of combinatorial
364 genetic manipulation of circadian clock and candidate 12h regulators in human cells/tissues *ex*
365 *vivo.*

366 Similar studies of molecular rhythms in model organisms typically require terminal tissue
367 collection and therefore require inclusion of several animals at each timepoint [12, 13]. Given the
368 genetic and environmental variability of free-living humans, analogous human studies have
369 required hundreds of participants [57]. Our study strength owes to the prospective, repeated
370 sample collection at high temporal resolution, which enabled high fidelity testing for a ~12h gene
371 program *within* each participant. Despite this strength, our study also demonstrates the challenge
372 of identifying specific rhythmic genes, as several canonical circadian genes did not meet statistical
373 significance in all participants. Even genes that are under rhythmic control may have additional

374 confounding regulatory inputs from environmental or behavioral stimuli and as such we propose
375 that functional relevance is enhanced by our pathway level analyses, which demonstrated
376 commonality of the putative ~12h pathways across all three human participants and their
377 conservation in organisms ranging from marine animals to humans. While these data provide
378 evidence in support of a ~12h gene program in humans, larger studies will be needed to determine
379 how variable the ~12h programs are in the human population, the degree to which they are
380 sensitive to aging or environmental stressors as observed for circadian rhythms, and most
381 importantly whether disruption of ~12h rhythms is a causal determinant of disease pathobiology.
382 Aside from the identification of ~12h pathways related to fundamental cellular processes, several
383 pieces of evidence suggest that ~12h rhythms are important for maintenance of homeostasis: (i)
384 when we adjusted for detection sensitivity by matching sampling frequency to period length , the
385 number of putative ~12h genes was similar to the circadian program; and (ii) prior human studies
386 suggest ~12h rhythms in physiological metrics of relevance to human health and disease,
387 including heart rate variability, blood pressure, hormone levels, and cognitive function [6, 8, 58,
388 59]. As such, our discovery of ancient ~12h gene programs in humans provides rationale for future
389 studies to determine whether ~12h rhythms should be viewed alongside circadian rhythms as a
390 core molecular determinant of health and disease.
391

392 **Materials and Methods**

393 **Human participants and study protocol**

394 The study protocol was approved by the University of Pittsburgh Institutional Review Board (Study
395 20020034; approval date: 6/4/2020) and written consent was obtained from all study participants.
396 We studied 3 healthy male participants, who were recruited through online advertisements.
397 Inclusion criteria consisted of individuals 18-35 years of age with a self-reported regular nighttime
398 sleep schedule and a body mass index between 18.5-24.9 kg/m^2. Volunteers were excluded if

399 they admitted to nighttime shift work or other regular nighttime sleep-disrupting activities, if they
400 had any chronic medical conditions, took any medications or recreational drugs, or used tobacco
401 products. Potential volunteers presented for a screening visit, inclusive of measurement of body
402 weight, height, BMI, and laboratory studies, including a comprehensive metabolic panel
403 (electrolytes, kidney function and liver function tests), complete blood count, 25-OH vitamin D,
404 and thyroid stimulating hormone level, to screen for potential subclinical chronic diseases. We
405 excluded participants with low hemoglobin/hematocrit, abnormal thyroid function and individuals
406 with 25-OH vitamin D < 20 ng/mL.

407 Qualifying study participants maintained a food diary, which was used to estimate their daily
408 caloric intake and subsequently presented to the University of Pittsburgh Medical Center (UPMC)
409 Clinical Translational Research Center (CTRC) for a 3-day inpatient visit. On the morning of
410 admission, participants selected items from a food menu designed to match their standard daily
411 caloric intake with a uniform macronutrient composition of 55% carbohydrates, 25% fat, 20%
412 protein per day. No interventions were performed during the first 24-hour period of acclimatization.

413 On the morning of the second day at 8am, an intravenous (IV) line was placed. Blood samples
414 were then collected every two hours for 48 hours (total 24 samples). Nighttime blood collection
415 was performed through a long IV line from outside the room so that the study participant would
416 not be exposed to light or woken up during blood collection. Blood was then immediately
417 processed in the Center for Human Integrative Physiology, two floors above the UPMC CTRC by
418 a rotating study team, all of whom were trained in the processing procedures for this study. Blood
419 was centrifuged (1900 RCF x 10 min) and the buffy coats were collected and immediately snap
420 frozen in liquid nitrogen for storage at -80C.

421 **RNA-Seq and data analysis**

422 RNA was isolated from peripheral blood buffy coat samples on the automated Chemagic 360
423 (Perkin Elmer) instrument according to the manufacturer's instructions. Extracted RNA was
424 quantitated by Qubit™ RNA BR Assay Kit (Thermo Fisher Scientific) followed by the RNA quality
425 check using Fragment Analyzer (Agilent). For each sample, RNA libraries were prepared from
426 100ng RNA using the KAPA RNA HyperPrep Kit with RiboErase (Kapa Biosystems) according to
427 manufacturer's protocol, followed by quality check using Fragment Analyzer (Agilent) and
428 quantification by qPCR (Kapa qPCR quantification kit, Kapa biosystem) on the LightCycler 480
429 (Roche). The libraries were normalized and pooled, and then sequenced using NovaSeq6000
430 platform (Illumina) to an average of 40M 101bp paired end reads per sample. Low-quality reads
431 and adapter sequences were trimmed from the raw sequencing data with Trimmomatic [60]. The
432 remaining reads were then aligned to human reference genome hg38 with STAR aligner [61].
433 Gene counts were quantified with the STAR-quantMode GeneCounts function. Fragments per
434 kilobase of transcript per million mapped fragments (FPKM) were quantified with Cufflinks [62].

435 **Identification of the oscillating transcriptome**

436 Averaged FPKM values at each time were used for cycling transcripts identification. Lowly
437 expressed transcripts were removed by calculating the background expression in each participant
438 using the average expression of a panel of 62 genes known not to be expressed in peripheral
439 blood cells (**Table S2**). Temporal transcriptomes were participant to linear detrend prior to
440 identification of oscillations by either the eigenvalue/pencil or RAIN methods. For the
441 eigenvalue/pencil method [10, 12], a maximum of four oscillations were identified for each gene.
442 Criterion for circadian genes were: period between 20h to 25h for first and second participants
443 and 24h to 30h for the third participant, decay rate between 0.8 and 1.2; for ~12h genes: period
444 between 9.6h to 13.6h for the second and third participants and 10h to 14h for the first participant,
445 decay rate between 0.8 and 1.2; for ~8h genes: period between 6h to 8h for the first participant
446 and 7h to 9h for the second participant, decay rate between 0.8 and 1.2; for ~16h genes; period

447 between 14h to 18h for the third participant. The relative amplitude was calculated by dividing the
448 amplitude by the mean expression value for each gene. To determine FDR, we used a
449 permutation-based method that randomly shuffles the time label of gene expression data and
450 subjected each permutation dataset to the eigenvalue/pencil method applied with the same
451 criterion [29]. These permutation tests were run 5,000 times, and FDR was estimated by taking
452 the ratio between the mean number of rhythmic profiles identified in the permutated samples
453 (false positives) and the number of rhythmic profiles identified in the original data. Analyses were
454 performed in MatlabR2017A. RAIN analysis was performed as previously described in
455 Bioconductor (3.4) (http://www.bioconductor.org/packages/release/bioc/html/rain.html) with
456 either 48h continuous data or 24h data with biological duplicates as input [11]. We included genes
457 exhibiting a period between 10h and 14h with a p value less than 0.05 as having ~12h expression
458 in all three participants. FDR was calculated using the Benjamini-Hochberg procedure. Heat maps
459 were generated with Gene Cluster 3.0 and TreeView 3.0 alpha 3.0 using Z score normalized
460 values.

461 For meta-analysis, we used Fisher's method, which combines extreme value probabilities from
462 each test, commonly known as "p-values", into one test statistic (X2) using the formula

463 $$X_{2k}^2 = -2\sum_{i=1}^{k} \ln p_i,$$

464 where pi is the p-value for the ith hypothesis test.

465 For RAIN analysis on temporal IR events and splicing gene expression, raw data was subjected
466 to polynomial detrend (n=2) before RAIN analysis.

467 **Defining oscillating genes**

468 The eigenvalue method can detect multiple superimposed oscillations. Therefore, we defined a
469 circadian gene as one that exhibited a circadian rhythm, regardless of its amplitude relative to
470 other superimposed oscillations. Similar criteria were applied to other oscillations. As such, a gene
471 can meet criteria for both a circadian and ~12h gene. By comparison, we define a dominant
472 circadian gene as one in which the superimposed circadian rhythm has the largest amplitude
473 among all oscillations. With this definition, dominant circadian and dominant 12h genes are
474 mutually exclusive.

475 **Intron retention detection**

476 Intron retention events were detected by tool iREAD [41]. Intron retention events are selected
477 either with default settings T>=20, J>=1, FPKM>=2 and NE score>=0.9 or more stringent settings
478 where T>=20, J>=1, FPKM>=3 and NE score>=0.9.

479 **Gene ontology analysis**

480 DAVID (Version 2021) [63] (https://david.ncifcrf.gov) was used to perform Gene Ontology
481 analyses. Briefly, gene names were first converted to DAVID-recognizable IDs using Gene
482 Accession Conversion Tool. The updated gene list was then subject to GO analysis using all
483 Homo Sapiens as background and with Functional Annotation Chart function. GO_BP_DIRECT,
484 KEGG_PATHWAY or UP_KW_BIOLOGICAL_PROCESS was used as GO categories. Only GO
485 terms with a p value less than 0.05 were included for further analysis.

486 **Motif analysis**

487 Motif analysis was performed with the SeqPos motif tool (version 0.590) embedded in Galaxy
488 Cistrome using all motifs within the homo sapiens reference genome hg19 as background. LISA
489 analysis was performed using webtool (http://lisa.cistrome.org/).

490 **Acknowledgments:**

We thank Toren Finkel for critical discussion and insightful advice on the manuscript, and Soukaina Eljamri for help with the human study protocols. This research was supported in part by the University of Pittsburgh Center for Research Computing through the resources provided. Specifically, this work used the HTC cluster, which is supported by NIH award number S10OD028483.

Funding:

Internal funds from the Center for Human Integrative Physiology, Aging Institute, University of Pittsburgh School of Medicine (PKF, MLS)

National Institute of Health grant DP2GM140924 (BZ)

National Institute of Health grant R21AG071893 (BZ)

National Institute of Health grant P30DK120531 (SL)

Author contributions:

Conceptualization: BZ, PKF, MLS

Methodology: BZ, SL, PKF, MLS

Investigation: BZ, SL, PKF, MLS, NLD, NKD, WD, LBS, TA, REA, GVNK, SI, TP, AXS, MS

Visualization: BZ, SL

Formal Analysis: BZ, SL, HL

Funding acquisition: BZ, PKF, MLS

Resources: BZ, PKF, MLS

Software: BZ, SL

Validation: BZ, SL

Supervision: BZ, PKF, MLS

Writing – original draft: BZ, SL, PKF, MLS

Writing – review & editing: all authors

Competing interests:

The authors declare no competing interests.

Data and materials availability:

All raw and processed sequencing data generated in this study have been submitted to the NCBI Gene Expression Omnibus (GEO; http://www.ncbi.nlm.nih.gov/geo/) under accession numbers GSE220120.

References

1. Bass J, Takahashi JS. Circadian integration of metabolism and energetics. Science. 2010;330(6009):1349-54. doi: 10.1126/science.1195027. PubMed PMID: 21127246; PubMed Central PMCID: PMC3756146.

2. Allada R, Bass J. Circadian Mechanisms in Medicine. New England Journal of Medicine. 2021;384(6):550-61. doi: 10.1056/NEJMra1802337. PubMed PMID: 33567194.

3. Czeisler CA, Johnson MP, Duffy JF, Brown EN, Ronda JM, Kronauer RE. Exposure to Bright Light and Darkness to Treat Physiologic Maladaptation to Night Work. New England Journal of Medicine. 1990;322(18):1253-9. doi: 10.1056/nejm199005033221801. PubMed PMID: 2325721.

4. Sack RL. Jet Lag. New England Journal of Medicine. 2010;362(5):440-7. doi: 10.1056/NEJMcp0909838. PubMed PMID: 20130253.

5. Andreatta G, Tessmar-Raible K. The Still Dark Side of the Moon: Molecular Mechanisms of Lunar-Controlled Rhythms and Clocks. J Mol Biol. 2020;432(12):3525-46. doi: 10.1016/j.jmb.2020.03.009. PubMed PMID: 32198116; PubMed Central PMCID: PMCPMC7322537.

6. Ballance H, Zhu B. Revealing the hidden reality of the mammalian 12-h ultradian rhythms. Cellular and Molecular Life Sciences. 2021. doi: 10.1007/s00018-020-03730-5.

7. Asher G, Zhu B. Beyond circadian rhythms: Emerging roles of ultradian rhythms in control of liver functions. Hepatology. 2022. Epub 2022/05/21. doi: 10.1002/hep.32580. PubMed PMID: 35591797.

8. Scott MR, Zong W, Ketchesin KD, Seney ML, Tseng GC, Zhu B, et al. Twelve-hour rhythms in transcript expression within the human dorsolateral prefrontal cortex are altered in schizophrenia. PLOS Biology. 2023;21(1):e3001688. doi: 10.1371/journal.pbio.3001688.

546 9. Zhu B, Dacso CC, O'Malley BW. Unveiling "Musica Universalis" of the Cell: A Brief
547 History of Biological 12-Hour Rhythms. J Endocr Soc. 2018;2(7):727-52. Epub 2018/07/07. doi:
548 10.1210/js.2018-00113. PubMed PMID: 29978151; PubMed Central PMCID:
549 PMCPMC6025213.

550 10. Antoulas AC, Zhu B, Zhang Q, York B, O'Malley BW, Dacso CC. A novel mathematical
551 method for disclosing oscillations in gene transcription: A comparative study. PLoS One.
552 2018;13(9):e0198503. Epub 2018/09/20. doi: 10.1371/journal.pone.0198503. PubMed PMID:
553 30231032; PubMed Central PMCID: PMCPMC6145530.

554 11. Thaben PF, Westermark PO. Detecting rhythms in time series with RAIN. J Biol
555 Rhythms. 2014;29(6):391-400. Epub 20141017. doi: 10.1177/0748730414553029. PubMed
556 PMID: 25326247; PubMed Central PMCID: PMCPMC4266694.

557 12. Zhu B, Zhang Q, Pan Y, Mace EM, York B, Antoulas AC, et al. A Cell-Autonomous
558 Mammalian 12 hr Clock Coordinates Metabolic and Stress Rhythms. Cell Metab.
559 2017;25(6):1305-19 e9. doi: 10.1016/j.cmet.2017.05.004. PubMed PMID: 28591634.

560 13. Pan Y, Ballance H, Meng H, Gonzalez N, Kim S-M, Abdurehman L, et al. 12-h clock
561 regulation of genetic information flow by XBP1s. PLOS Biology. 2020;18(1):e3000580. doi:
562 10.1371/journal.pbio.3000580.

563 14. Wittenbrink N, Ananthasubramaniam B, Münch M, Koller B, Maier B, Weschke C, et al.
564 High-accuracy determination of internal circadian time from a single blood sample. J Clin Invest.
565 2018;128(9):3826-39. doi: 10.1172/JCI120874.

566 15. Yoon S, Baik B, Park T, Nam D. Powerful p-value combination methods to detect
567 incomplete association. Scientific Reports. 2021;11(1):6980. doi: 10.1038/s41598-021-86465-y.

568 16. Korf-Klingebiel M, Reboll MR, Klede S, Brod T, Pich A, Polten F, et al. Myeloid-derived
569 growth factor (C19orf10) mediates cardiac repair following myocardial infarction. Nature
570 medicine. 2015;21(2):140-9.

571 17. Bortnov V, Tonelli M, Lee W, Lin Z, Annis DS, Demerdash ON, et al. Solution structure
572 of human myeloid-derived growth factor suggests a conserved function in the endoplasmic
573 reticulum. Nature Communications. 2019;10(1):5612. doi: 10.1038/s41467-019-13577-5.

574 18. Borini Etichetti C, Di Benedetto C, Rossi C, Baglioni MV, Bicciato S, Del Sal G, et al.
575 Isoprenylcysteine carboxy methyltransferase (ICMT) is associated with tumor aggressiveness
576 and its expression is controlled by the p53 tumor suppressor. Journal of Biological Chemistry.
577 2019;294(13):5060-73. doi: https://doi.org/10.1074/jbc.RA118.006037.

578 19. Telesio G, Scudiero I, Pizzulo M, Mazzone P, Zotti T, Voccola S, et al. The E3 Ubiquitin
579 Ligase RNF7 Negatively Regulates CARD14/CARMA2sh Signaling. Int J Mol Sci. 2017;18(12).
580 Epub 20171201. doi: 10.3390/ijms18122581. PubMed PMID: 29194363; PubMed Central
581 PMCID: PMCPMC5751184.

582 20. Hakimi AA, Tickoo SK, Jacobsen A, Sarungbam J, Sfakianos JP, Sato Y, et al. TCEB1-
583 mutated renal cell carcinoma: a distinct genomic and morphological subtype. Modern Pathology.
584 2015;28(6):845-53. doi: 10.1038/modpathol.2015.6.

585 21. Bonnefoy N, Kermorgant M, Groudinsky O, Minet M, Slonimski PP, Dujardin G. Cloning
586 of a human gene involved in cytochrome oxidase assembly by functional complementation of an
587 oxa1- mutation in Saccharomyces cerevisiae. Proc Natl Acad Sci U S A. 1994;91(25):11978-82.
588 doi: 10.1073/pnas.91.25.11978. PubMed PMID: 7991568; PubMed Central PMCID:
589 PMCPMC45359.

590 22. Otera H, Wang C, Cleland MM, Setoguchi K, Yokota S, Youle RJ, et al. Mff is an
591 essential factor for mitochondrial recruitment of Drp1 during mitochondrial fission in mammalian
592 cells. J Cell Biol. 2010;191(6):1141-58. doi: 10.1083/jcb.201007152. PubMed PMID: 21149567;
593 PubMed Central PMCID: PMCPMC3002033.

594 23. van der Veen DR, Gerkema MP. Unmasking ultradian rhythms in gene expression. The
595 FASEB Journal. 2017;31(2):743-50. doi: https://doi.org/10.1096/fj.201600872R.

596 24. Kembro JM, Flesia AG, Nieto PS, Caliva JM, Lloyd D, Cortassa S, et al. A dynamically
597 coherent pattern of rhythms that matches between distant species across the evolutionary
598 scale. Scientific Reports. 2023;13(1):5326. doi: 10.1038/s41598-023-32286-0.

599 25. Hughes ME, DiTacchio L, Hayes KR, Vollmers C, Pulivarthy S, Baggs JE, et al.
600 Harmonics of circadian gene transcription in mammals. PLoS Genet. 2009;5(4):e1000442. doi:
601 10.1371/journal.pgen.1000442. PubMed PMID: 19343201; PubMed Central PMCID:
602 PMC2654964.

603 26. Meng H, Gonzales NM, Lonard DM, Putluri N, Zhu B, Dacso CC, et al. XBP1 links the
604 12-hour clock to NAFLD and regulation of membrane fluidity and lipid homeostasis. Nature
605 Communications. 2020;11(1):6215. doi: 10.1038/s41467-020-20028-z.

606 27. Dion W, Ballance H, Lee J, Pan Y, Irfan S, Edwards C, et al. Four-dimensional nuclear
607 speckle phase separation dynamics regulate proteostasis. Science Advances.
608 2022;8(1):eabl4150. doi: doi:10.1126/sciadv.abl4150.

609 28. Meng H, Gonzales NM, Jung SY, Lu Y, Putluri N, Zhu B, et al. Defining the mammalian
610 coactivation of hepatic 12-h clock and lipid metabolism. Cell Reports. 2022;38(10):110491. doi:
611 https://doi.org/10.1016/j.celrep.2022.110491.

612 29. Rey G, Milev NB, Valekunja UK, Ch R, Ray S, Silva Dos Santos M, et al. Metabolic
613 oscillations on the circadian time scale in Drosophila cells lacking clock genes. Mol Syst Biol.
614 2018;14(8):e8376. Epub 2018/08/04. doi: 10.15252/msb.20188376. PubMed PMID: 30072421;
615 PubMed Central PMCID: PMCPMC6078164.

616 30. Qin Q, Fan J, Zheng R, Wan C, Mei S, Wu Q, et al. Lisa: inferring transcriptional
617 regulators through integrative modeling of public chromatin accessibility and ChIP-seq data.
618 Genome Biology. 2020;21(1):32. doi: 10.1186/s13059-020-1934-6.

619 31. Zhang R, Misra V. Effects of cyclic AMP response element binding protein-Zhangfei
620 (CREBZF) on the unfolded protein response and cell growth are exerted through the tumor
621 suppressor p53. Cell Cycle. 2014;13(2):279-92. Epub 20131118. doi: 10.4161/cc.27053.
622 PubMed PMID: 24200963; PubMed Central PMCID: PMCPMC3906244.

623 32. Zhang R, Rapin N, Ying Z, Shklanka E, Bodnarchuk TW, Verge VMK, et al.
624 Zhangfei/CREB-ZF – A Potential Regulator of the Unfolded Protein Response. PLOS ONE.
625 2013;8(10):e77256. doi: 10.1371/journal.pone.0077256.

626 33. Kikuchi D, Tanimoto K, Nakayama K. CREB is activated by ER stress and modulates the
627 unfolded protein response by regulating the expression of IRE1α and PERK. Biochem Biophys
628 Res Commun. 2016;469(2):243-50. Epub 20151128. doi: 10.1016/j.bbrc.2015.11.113. PubMed
629 PMID: 26642955.

630 34. Sriburi R, Jackowski S, Mori K, Brewer JW. XBP1 : a link between the unfolded
631 protein response, lipid biosynthesis, and biogenesis of the endoplasmic reticulum. Journal of
632 Cell Biology. 2004;167(1):35-41. doi: 10.1083/jcb.200406136.

633 35. Li Y, Yip WK, Penney J, Taylor T, Zhang Y, Zeng M, et al. A CREBZF/Zhangfei isoform
634 activates CHOP during prolonged cellular stress. bioRxiv. 2022:2022.10.10.511668. doi:
635 10.1101/2022.10.10.511668.

636 36. Yang ZF, Drumea K, Mott S, Wang J, Rosmarin AG. GABP transcription factor (nuclear
637 respiratory factor 2) is required for mitochondrial biogenesis. Mol Cell Biol. 2014;34(17):3194-
638 201. Epub 20140623. doi: 10.1128/mcb.00492-12. PubMed PMID: 24958105; PubMed Central
639 PMCID: PMCPMC4135556.

640 37. Mootha VK, Handschin C, Arlow D, Xie X, St Pierre J, Sihag S, et al. Erralpha and
641 Gabpa/b specify PGC-1alpha-dependent oxidative phosphorylation gene expression that is
642 altered in diabetic muscle. Proc Natl Acad Sci U S A. 2004;101(17):6570-5. Epub 20040420.
643 doi: 10.1073/pnas.0401401101. PubMed PMID: 15100410; PubMed Central PMCID:
644 PMCPMC404086.

645 38. Pramanik J, Chen X, Kar G, Henriksson J, Gomes T, Park JE, et al. Genome-wide
646 analyses reveal the IRE1a-XBP1 pathway promotes T helper cell differentiation by resolving
647 secretory stress and accelerating proliferation. Genome Med. 2018;10(1):76. doi:
648 10.1186/s13073-018-0589-3. PubMed PMID: 30355343; PubMed Central PMCID:
649 PMCPMC6199730.

650 39. Zhu B. Decoding the function and regulation of the mammalian 12h-clock. Journal of
651 Molecular Cell Biology. 2020. doi: 10.1093/jmcb/mjaa021.

652 40. Pramanik J, Chen X, Kar G, Henriksson J, Gomes T, Park J-E, et al. Genome-wide
653 analyses reveal the IRE1a-XBP1 pathway promotes T helper cell differentiation by resolving
654 secretory stress and accelerating proliferation. Genome Medicine. 2018;10(1):76. doi:
655 10.1186/s13073-018-0589-3.

656 41. Li H-D, Funk CC, Price ND. iREAD: a tool for intron retention detection from RNA-seq
657 data. BMC Genomics. 2020;21(1):128. doi: 10.1186/s12864-020-6541-0.

658 42. Castellana S, Mazza T, Capocefalo D, Genov N, Biagini T, Fusilli C, et al. Systematic
659 Analysis of Mouse Genome Reveals Distinct Evolutionary and Functional Properties Among
660 Circadian and Ultradian Genes. Front Physiol. 2018;9:1178. doi: 10.3389/fphys.2018.01178.
661 PubMed PMID: 30190679; PubMed Central PMCID: PMCPMC6115496.

662 43. Schnytzer Y, Simon-Blecher N, Li J, Ben-Asher HW, Salmon-Divon M, Achituv Y, et al.
663 Tidal and diel orchestration of behaviour and gene expression in an intertidal mollusc. Scientific
664 Reports. 2018;8(1):4917. doi: 10.1038/s41598-018-23167-y.

665 44. Sorek M, Schnytzer Y, Ben-Asher HW, Caspi VC, Chen CS, Miller DJ, et al. Setting the
666 pace: host rhythmic behaviour and gene expression patterns in the facultatively symbiotic
667 cnidarian Aiptasia are determined largely by Symbiodinium. Microbiome. 2018;6(1):83. Epub
668 2018/05/10. doi: 10.1186/s40168-018-0465-9. PubMed PMID: 29739445; PubMed Central
669 PMCID: PMCPMC5941691.

670 45. Rinsky M, Weizman E, Ben-Asher HW, Eyal G, Zhu B, Levy O. Temporal gene
671 expression patterns in the coral Euphyllia paradivisa reveal the complexity of biological clocks in
672 the cnidarian-algal symbiosis. Science Advances. 2022;8(37):eabo6467.

673 46. Yokomizo T, Takahashi Y. Plasticity of circadian and circatidal rhythms in activity and
674 transcriptomic dynamics in a freshwater snail. bioRxiv. 2023:2023.08.19.553957. doi:
675 10.1101/2023.08.19.553957.

676 47. Sorek M, Schnytzer Y, Waldman Ben-Asher H, Caspi VC, Chen C-S, Miller DJ, et al.
677 Setting the pace: host rhythmic behaviour and gene expression patterns in the facultatively
678 symbiotic cnidarian Aiptasia are determined largely by Symbiodinium. Microbiome.
679 2018;6(1):83. doi: 10.1186/s40168-018-0465-9.

680 48. Putnam NH, Srivastava M, Hellsten U, Dirks B, Chapman J, Salamov A, et al. Sea
681 anemone genome reveals ancestral eumetazoan gene repertoire and genomic organization.
682 Science. 2007;317(5834):86-94. doi: 10.1126/science.1139158. PubMed PMID: 17615350.

683 49. Rodríguez-González C, Lin S, Arkan S, Hansen C. Co-chaperones DNAJA1 and
684 DNAJB6 are critical for regulation of polyglutamine aggregation. Scientific Reports.
685 2020;10(1):8130. doi: 10.1038/s41598-020-65046-5.

686 50. Adams BM, Canniff NP, Guay KP, Larsen ISB, Hebert DN. Quantitative glycoproteomics
687 reveals cellular substrate selectivity of the ER protein quality control sensors UGGT1 and
688 UGGT2. eLife. 2020;9:e63997. doi: 10.7554/eLife.63997.

689 51. Boye E, Grallert B. eIF2α phosphorylation and the regulation of translation. Curr Genet.
690 2020;66(2):293-7. Epub 20190904. doi: 10.1007/s00294-019-01026-1. PubMed PMID:
691 31485739.

692 52. Cretenet G, Le Clech M, Gachon F. Circadian clock-coordinated 12 Hr period rhythmic
693 activation of the IRE1alpha pathway controls lipid metabolism in mouse liver. Cell Metab.
694 2010;11(1):47-57. doi: 10.1016/j.cmet.2009.11.002. PubMed PMID: 20074527.

695 53. Hughes ME, Hong HK, Chong JL, Indacochea AA, Lee SS, Han M, et al. Brain-specific
696 rescue of Clock reveals system-driven transcriptional rhythms in peripheral tissue. PLoS Genet.
697 2012;8(7):e1002835. doi: 10.1371/journal.pgen.1002835. PubMed PMID: 22844252; PubMed
698 Central PMCID: PMC3405989.

699 54. Westermark PO, Herzel H. Mechanism for 12 hr rhythm generation by the circadian
700 clock. Cell Rep. 2013;3(4):1228-38. doi: 10.1016/j.celrep.2013.03.013. PubMed PMID:
701 23583178.

55. Zhu B, Liu S. Preservation of ~12-h ultradian rhythms of gene expression of mRNA and protein metabolism in the absence of canonical circadian clock. Frontiers in Physiology. 2023;14. doi: 10.3389/fphys.2023.1195001.

56. Dion W, Ballance H, Lee J, Pan Y, Irfan S, Edwards C, et al. Four-dimensional nuclear speckle phase separation dynamics regulate proteostasis. Science Advances. 2022;8(1):eabl4150.

57. Talamanca L, Gobet C, Naef F. Sex-dimorphic and age-dependent organization of 24-hour gene expression rhythms in humans. Science. 2023;379(6631):478-83. doi: doi:10.1126/science.add0846.

58. Otsuka K, Cornelissen G, Kubo Y, Shibata K, Mizuno K, Aiba T, et al. Methods for assessing change in brain plasticity at night and psychological resilience during daytime between repeated long-duration space missions. Scientific Reports. 2023;13(1):10909. doi: 10.1038/s41598-023-36389-6.

59. Otsuka K, Murakami S, Okajima K, Shibata K, Kubo Y, Gubin DG, et al. Appropriate Circadian-Circasemidian Coupling Protects Blood Pressure from Morning Surge and Promotes Human Resilience and Wellbeing. Clinical Interventions in Aging. 2023;18(null):755-69. doi: 10.2147/CIA.S398957.

60. Bolger AM, Lohse M, Usadel B. Trimmomatic: a flexible trimmer for Illumina sequence data. Bioinformatics. 2014;30(15):2114-20. doi: 10.1093/bioinformatics/btu170.

61. Dobin A, Davis CA, Schlesinger F, Drenkow J, Zaleski C, Jha S, et al. STAR: ultrafast universal RNA-seq aligner. Bioinformatics. 2013;29(1):15-21. Epub 20121025. doi: 10.1093/bioinformatics/bts635. PubMed PMID: 23104886; PubMed Central PMCID: PMCPMC3530905.

62. Trapnell C, Roberts A, Goff L, Pertea G, Kim D, Kelley DR, et al. Differential gene and transcript expression analysis of RNA-seq experiments with TopHat and Cufflinks. Nature Protocols. 2012;7(3):562-78. doi: 10.1038/nprot.2012.016.

63. Huang da W, Sherman BT, Lempicki RA. Systematic and integrative analysis of large gene lists using DAVID bioinformatics resources. Nat Protoc. 2009;4(1):44-57. doi: 10.1038/nprot.2008.211. PubMed PMID: 19131956.

739 **Figure and Table Legends**

740 **Table 1. Participant characteristics.**

	Participant 1	Participant 2	Participant 3
Age (years)	20	22	28
Body mass index (kg/m^2)	23.3	23.7	24.4
Vitamin D (ng/mL)	85	26	22
Glucose (mg/dL)	73	84	74
BUN (mg/dL)	10	18	14
Creatinine (mg/dL)	0.9	1.0	0.9
AST (U/L)	22	41	22
ALT (U/L)	10	28	22
TSH (mIU/L)	1.306	1.48	0.803

741
742
743
744

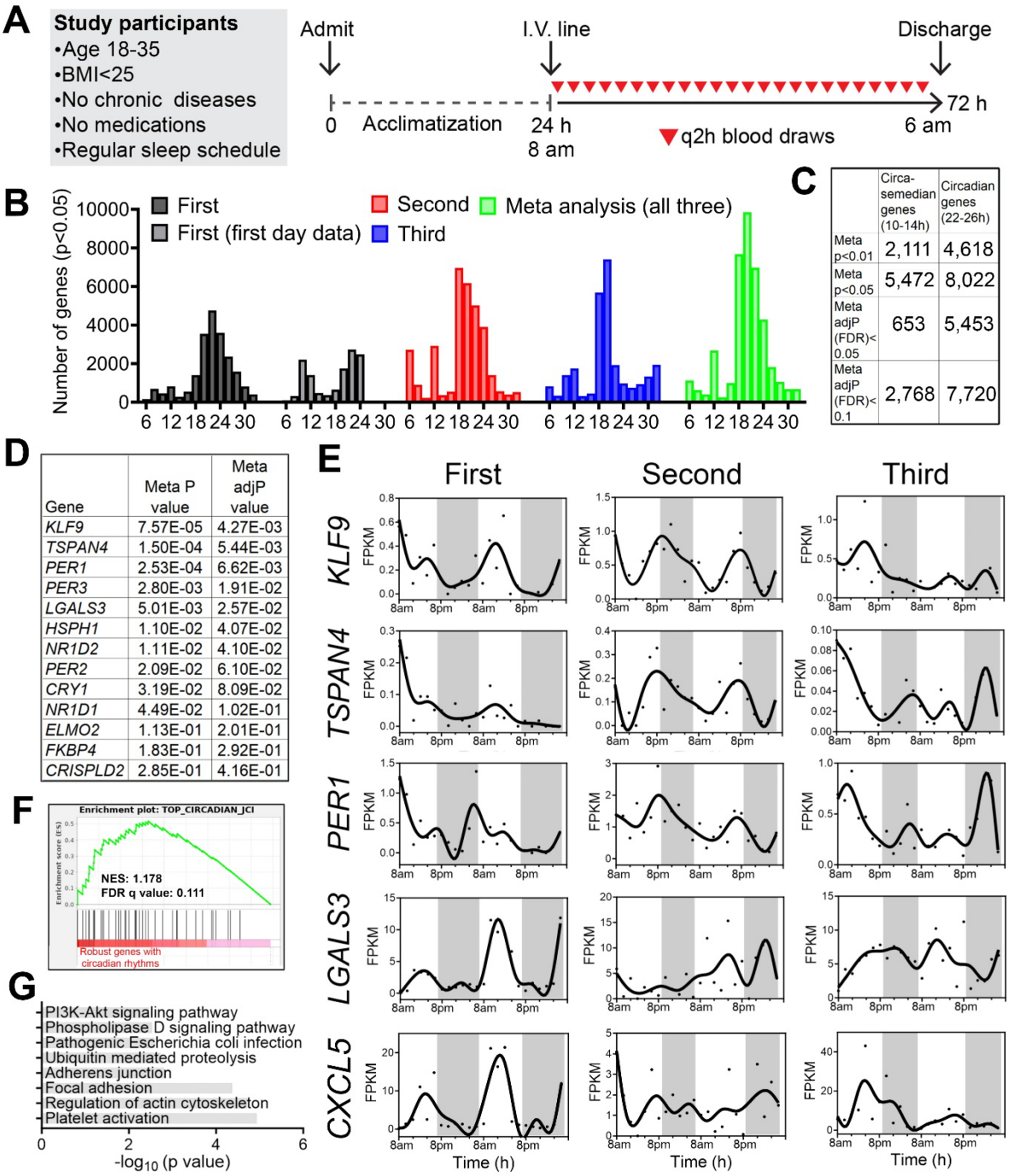

	Circa-semedian genes (10-14h)	Circadian genes (22-26h)
Meta p<0.01	2,111	4,618
Meta p<0.05	5,472	8,022
Meta adjP (FDR)< 0.05	653	5,453
Meta adjP (FDR)< 0.1	2,768	7,720

Gene	Meta P value	Meta adjP value
KLF9	7.57E-05	4.27E-03
TSPAN4	1.50E-04	5.44E-03
PER1	2.53E-04	6.62E-03
PER3	2.80E-03	1.91E-02
LGALS3	5.01E-03	2.57E-02
HSPH1	1.10E-02	4.07E-02
NR1D2	1.11E-02	4.10E-02
PER2	2.09E-02	6.10E-02
CRY1	3.19E-02	8.09E-02
NR1D1	4.49E-02	1.02E-01
ELMO2	1.13E-01	2.01E-01
FKBP4	1.83E-01	2.92E-01
CRISPLD2	2.85E-01	4.16E-01

Fig. 1. Identification of inter-individual variability of circadian and ultradian rhythms of gene expression in peripheral white blood cells of humans. (**A**) Human protocol and study schematic. (**B-D**) Histograms showing the period distributions of all rhythmic genes uncovered from the three participants (with p value<0.05) as well as the period distribution of rhythmic genes calculated by the meta p values (meta p<0.05). For the first individual, periods calculated from all 48 hours of data or the first 24h hours of the dataset were both shown. (**C**) Table summarizing the number of circadian and ~12h genes with different statistical cut-offs. (**D**) Table listing the meta P and meta adj-P (FDR) values of thirteen circadian genes previously used as training

754 dataset for predicting circadian phase from human blood samples [14]. (**E**) Raw temporal
755 expression profile (dot) and spline fit (solid line) of five of the thirteen circadian genes. (**F**) Gene
756 set enrichment analysis (GSEA) showing enrichment of a previously identified set of top forty
757 robustly-cycling circadian genes in human white blood cells [14] with robust circadian rhythmicity
758 in our study. (**G**) GO analyses of top KEGG pathways for circadian genes with meta adj-P (FDR)
759 less than 0.01.
760
761
762
763
764
765
766
767
768
769
770
771
772
773
774
775
776
777
778
779
780
781

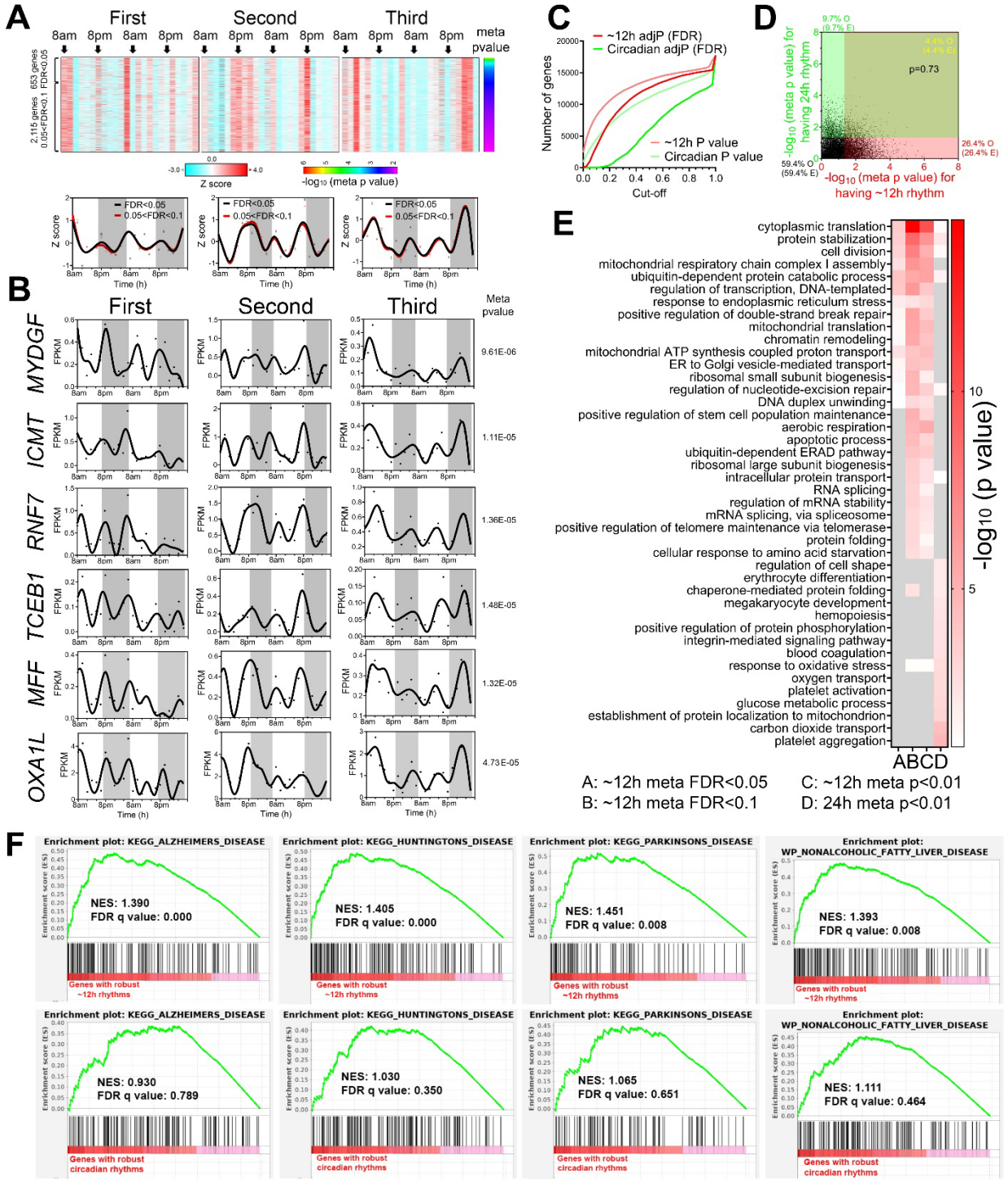

Fig. 2. ~12h gene expression rhythms are enriched in mRNA and protein homeostasis pathways. (**A**) Heatmap and quantification of ~12h genes from all three participants with meta adj-P (FDR) values less than 0.05 or between 0.05 and 0.1. (**B**) Raw temporal expression (dot) profile and spline fit (solid line) of six ~12h genes with meta p values also shown. (**C**) Cumulative distribution of the number of circadian and ~12h genes with different meta p and meta adj-P cut-

offs. The circadian data set consisted of a 4h sampling interval so that the period to sampling interval was matched to the ~12h data set. (**D**) Scatter plot comparing log transformed meta p values for each gene exhibiting circadian versus ~12h rhythms. Both observed and predicted percentage of genes (under the null hypothesis that ~12h and circadian genes are independently regulated) with meta p value smaller or larger than 0.05 are further shown. P value of 0.73 is calculated by Chi-square test. (**E**) GO analysis of circadian and ~12h genes with different statistical cut-offs. (**F**) GSEA showing enrichment scores of different gene sets for ~12h (top) and circadian (bottom) genes.

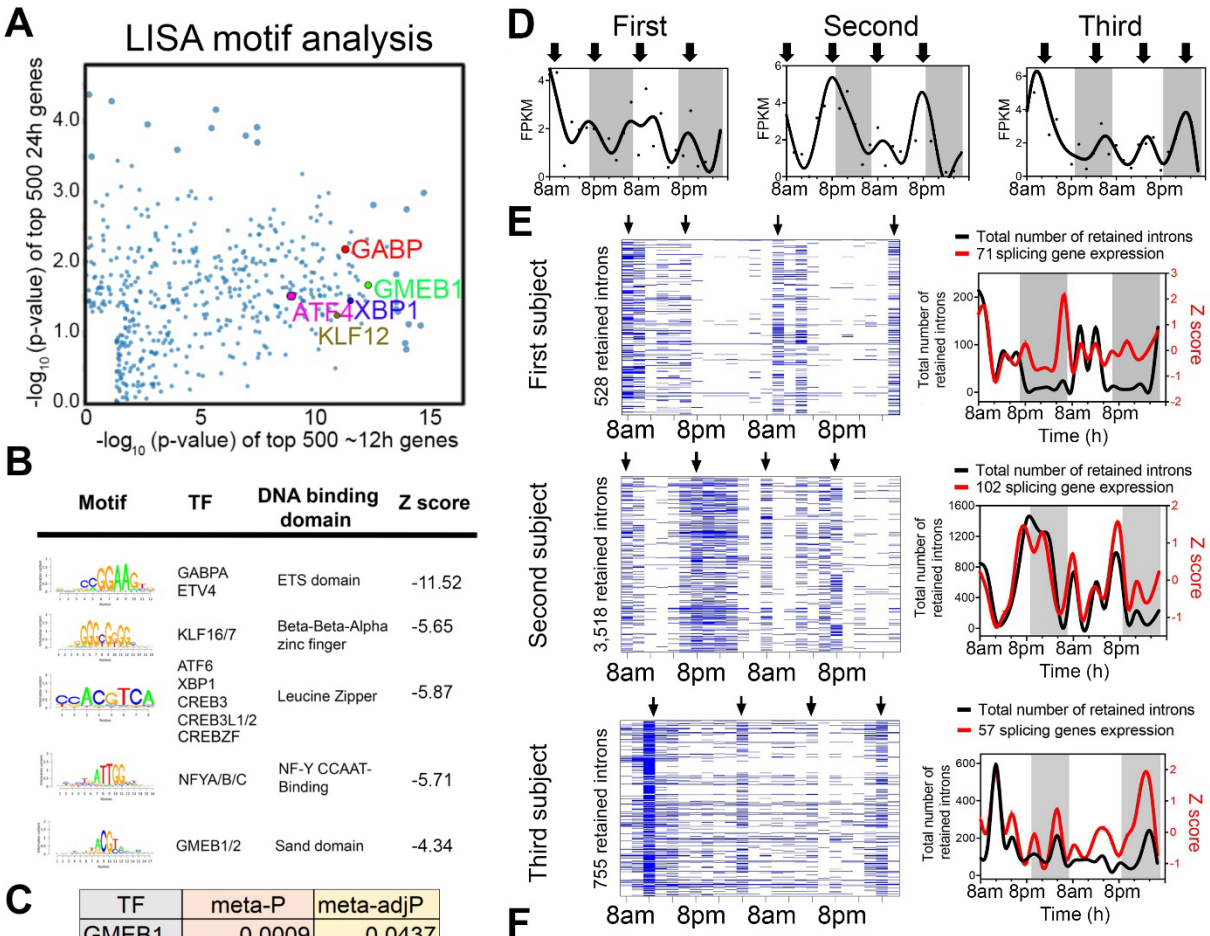

C

TF	meta-P	meta-adjP
GMEB1	0.0009	0.0437
GABPB1	0.0018	0.0498
CREBZF	0.0019	0.0510
XBP1	0.0029	0.0583
KLF16	0.0045	0.0658
NFYB	0.0073	0.0768
ETV6	0.0127	0.0916
CREB1	0.0132	0.0933
GABPB2	0.0143	0.0966

	Intron retention events rhythms		Splicing gene expression rhythms	
	Period	p value	Period	p value
First	10h	0.1911	12h	0.0546
Second	12h	0.0529	12h	0.0213
Third	12h	0.0013	12h	0.0015
Meta	10-12h	9.877E-04	12h	1.7716E-04

Fig. 3. Regulatory and functional dissection of human ~12h rhythms. (**A**) Scatter plot demonstrating the log normalized p values of motifs identified for top 500 (ranked by meta p values) ~12h (x axis) versus the circadian genes using the LISA program, with selective TFs highlighted. (**B**) Top motifs enriched at the promoters of ~top 500 12h genes using the SeqPos motif tool in Galaxy/Cistrome. (**C**) A table listing the TFs whose motifs are enriched in the promoters of ~12h genes and whose gene expression also exhibit ~12h rhythms with meta adj-P less than 0.1. (**D**) Temporal expression of *XBP1* in all three individuals. (**E, F**) Criterions for IR are set as T>=20, J>=1, FPKM>=2 and NE score>=0.9. Heatmap (left) and quantification (right) of temporal intron retention events, superimposed with the Z score normalized temporal expression of splicing genes exhibiting ~12h rhythms (**E**). Statistics for IR and spicing gene expression ~12h rhythms detection by RAIN (**F**).

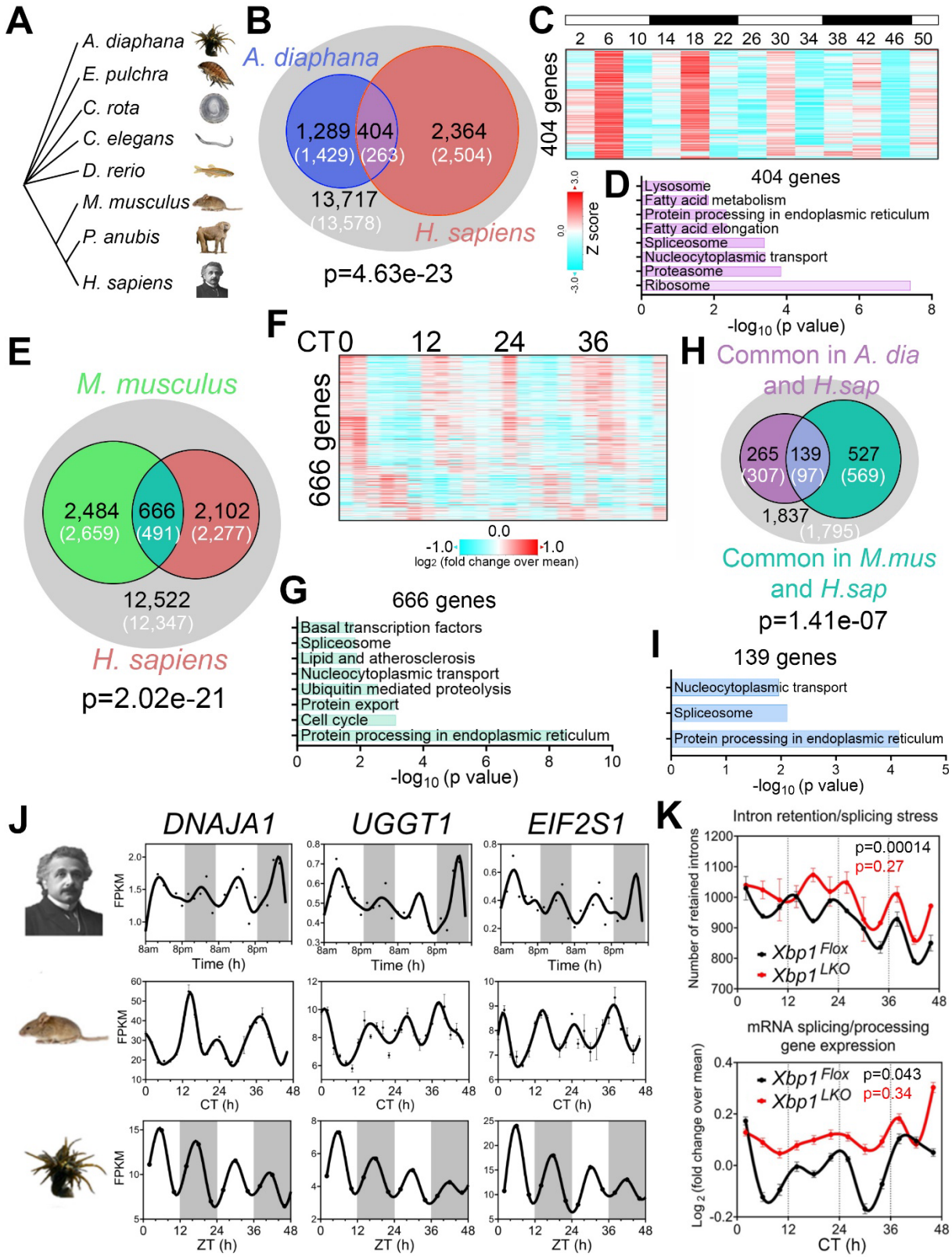
A
A. diaphana
E. pulchra
C. rota
C. elegans
D. rerio
M. musculus
P. anubis
H. sapiens
B
A. diaphana
1,289 (1,429)
404 (263)
2,364 (2,504)
13,717 (13,578)
H. sapiens
p=4.63e-23
C
404 genes
Z score
D
404 genes
Lysosome
Fatty acid metabolism
Protein processing in endoplasmic reticulum
Fatty acid elongation
Spliceosome
Nucleocytoplasmic transport
Proteasome
Ribosome
-log10 (p value)
E
M. musculus
2,484 (2,659)
666 (491)
2,102 (2,277)
12,522 (12,347)
H. sapiens
p=2.02e-21
F
CT0 12 24 36
666 genes
log2 (fold change over mean)
G
666 genes
Basal transcription factors
Spliceosome
Lipid and atherosclerosis
Nucleocytoplasmic transport
Ubiquitin mediated proteolysis
Protein export
Cell cycle
Protein processing in endoplasmic reticulum
-log10 (p value)
H
Common in A. dia and H.sap
265 (307)
139 (97)
527 (569)
1,837 (1,795)
Common in M.mus and H.sap
p=1.41e-07
I
139 genes
Nucleocytoplasmic transport
Spliceosome
Protein processing in endoplasmic reticulum
-log10 (p value)
J
DNAJA1
UGGT1
EIF2S1
FPKM
Time (h)
CT (h)
ZT (h)
K
Intron retention/splicing stress
Number of retained introns
p=0.00014
p=0.27
Xbp1 Flox
Xbp1 LKO
mRNA splicing/processing gene expression
Log2 (fold change over mean)
p=0.043
p=0.34
CT (h)

825

826 **Fig. 4. Evolutionary conservation of ~12h gene programs.** (**A**) Phylogenetic tree of select
827 species for which ~12h rhythms of gene expression have been demonstrated. *A. diaphana* is the
828 most distant from *H. sapiens*. (**B**) Venn diagram comparing distinct and shared ~12h genes in
829 human (meta adj-P<0.1) and *A. diaphana* (reported in [44]). Only genes expressed in human
830 white blood cells (denoted by the grey circle) are included in the analysis. Both observed and
831 predicted number of genes (under the null hypothesis that ~12h genes are not evolutionarily
832 conserved and thus independently detected in these two species) are further shown. P value of
833 4.6e-23 is calculated by Chi-square test. (**C, D**) Heatmap of temporal expression (Z score
834 normalized) of 404 circatidal genes in *A. diaphana* (**C**) and GO analysis of the top enriched
835 pathways (**D**). (**E**) Venn diagram comparing distinct and shared ~12h genes in human (meta adj-
836 P<0.1) and mouse liver (reported in [13]). Only genes that are expressed in human white blood
837 cells (denoted by the grey circle) are included in the analysis. Both observed and predicted
838 number of genes (under the null hypothesis that ~12h genes are not evolutionarily conserved and
839 thus independently detected in these two species) are further shown. P value of 2.0e-21 is
840 calculated by Chi-square test. (**F, G**) Heatmap of temporal expression (log 2 normalized) of 666
841 ~12h genes in mouse liver (**F**) and GO analysis of the top enriched pathways (**G**). (**H**) Venn
842 diagram further comparing the overlap of commonly identified 404 ~12h genes in human and A.
843 diaphana, and 666 ~12h genes in human and mouse. Both observed and predicted number of
844 genes (under the null hypothesis that ~12h genes are not evolutionarily conserved and thus
845 independently detected in all three species) are further shown. P value of 1.4e-7 is calculated by
846 Chi-square test. (**I**) GO analysis of the top enriched pathways of 139 ~12h genes commonly
847 identified in all three species. (**J**) Representative temporal expression of evolutionarily conserved
848 ~12h genes in human, mouse, and *A. diaphana*. (**K**) ~12h rhythms of intron retention events (top)
849 and RNA splicing genes expression (bottom) are attenuated by liver specific loss of function of
850 XBP1 ($Xbp1^{LKO}$: red), relative to control ($Xbp1^{Flox}$: black) in mice. P values calculated by RAIN for
851 12h rhythms.

852

853

854

855

856

857

858

859

860

Supplementary Materials for

Conservation of a primordial 12-hour ultradian gene program in humans

Bokai Zhu[1,2,3] *, Silvia Liu[2,4], Natalie L. David[1,5,6], William Dion[1], Nandini K Doshi[1,6], Lauren B. Siegel[5], Tânia Amorim[1,5,6], Rosemary E. Andrews[1,6], GV Naveen Kumar[1], Hanwen Li[7], Saad Irfan[1], Tristan Pesaresi[1,6], Ankit X. Sharma[1], Michelle Sun[1], Pouneh K. Fazeli [5,6] and Matthew L. Steinhauser [1,6,8] *

Corresponding author: bzhu@pitt.edu, msteinhauser@pitt.edu

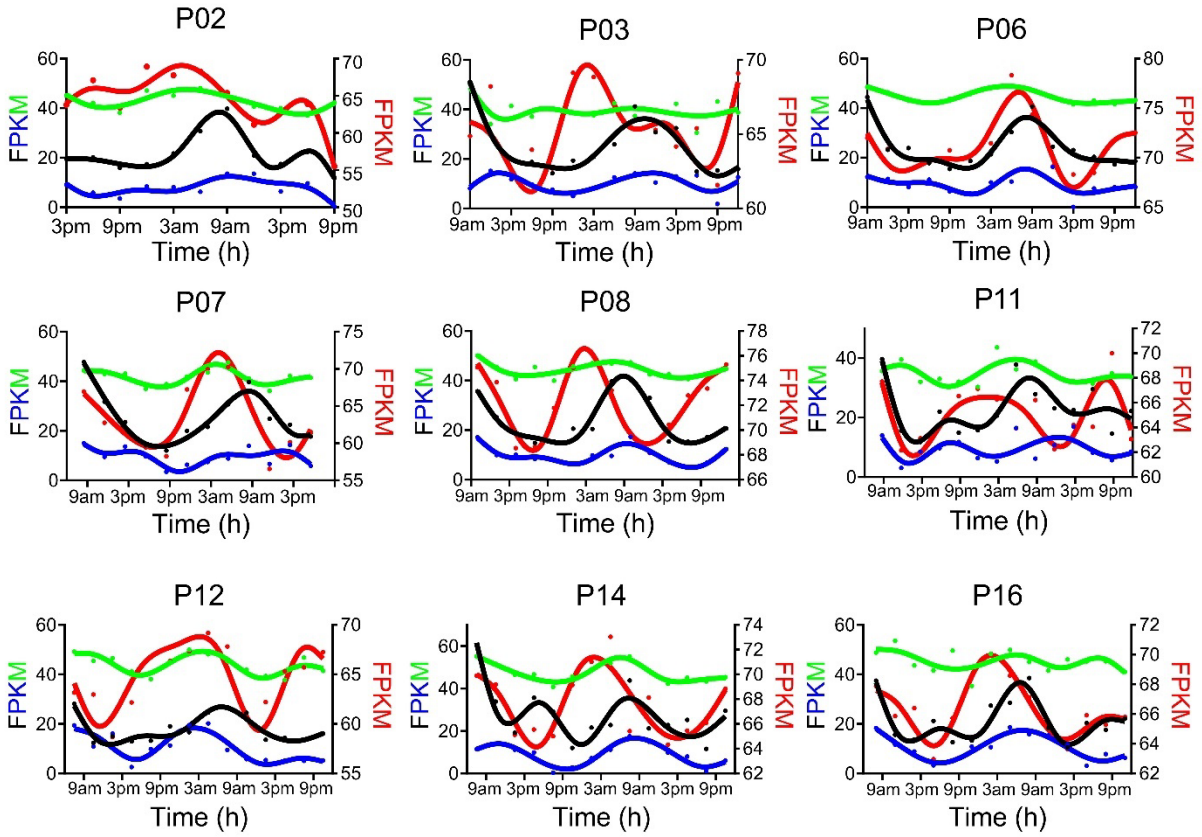

Fig. S1. Inter-individual variability of circadian rhythms of gene expression reported in the Wittenbrink et al JCI study. Raw temporal expression profile (dot) and spline fit (solid line) of *PER1* (black), *PER2* (blue), *TSPAN4* (green) and *LGALS3* (red) genes in nine different individuals, reported in [14].

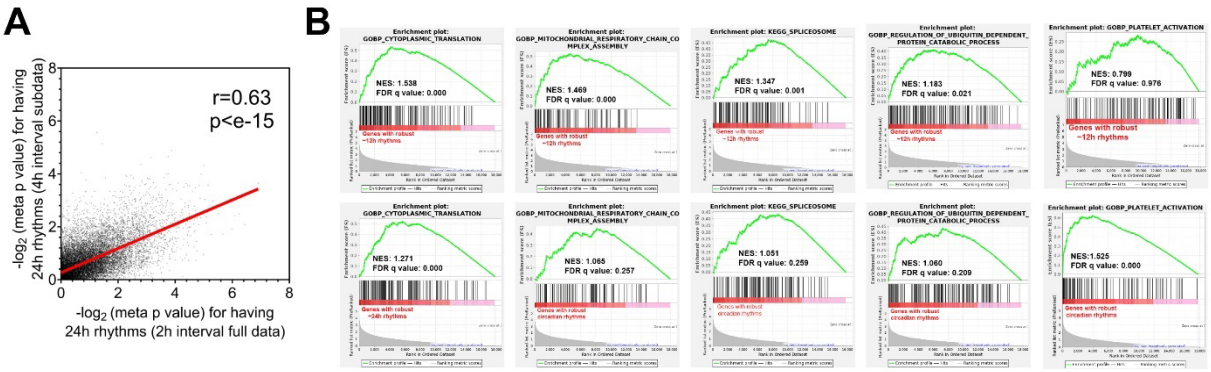

Fig. S2. Genes with ~12h and circadian rhythms are enriched in distinct biological pathways. (**A**) Scatter plot comparing log normalized meta p values for having circadian rhythms for each gene when the full 2h sampling interval dataset (x-axis) or the 4h sampling interval subset (y-axis) was used for the analysis. (**B**) GSEA showing enrichment scores for different gene sets in ~12h (top) and circadian (bottom) genes.

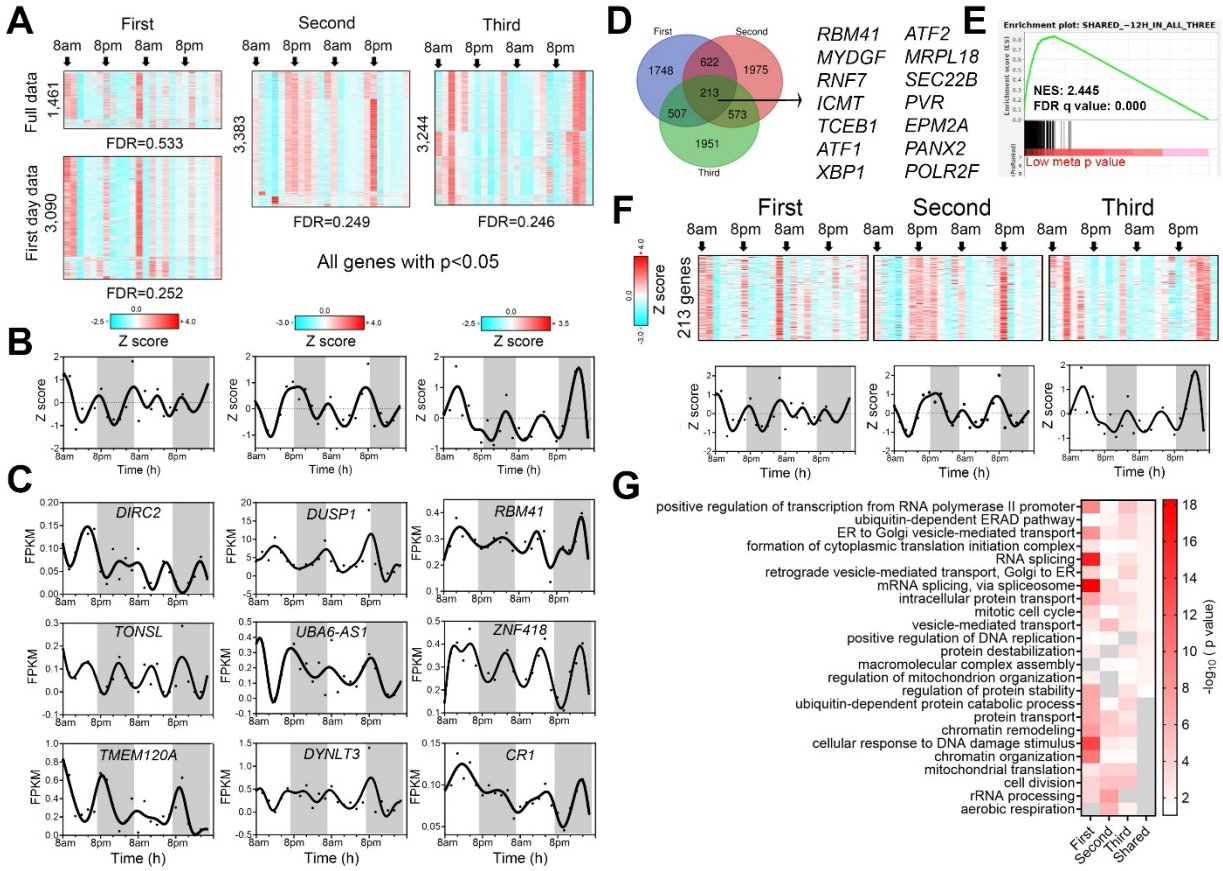

Fig. S3. RAIN analyses of 48h temporal transcriptome to detect ~12h genes. A single data point was inputted for each sample collected over the 48h protocol. (**A**) Heatmap of ~12h genes from all three participants with respective p values smaller than 0.05. The identification of a greater number of ~12h genes with lower FDR in the first participant with restriction of inputted data to the first 24 hours indicates the ~12h rhythm is dampened in the second day in this participant, consistent with what was found with the eigenvalue/pencil method. (**B**) Quantification of the average expression (Z score normalized) of genes shown in A, with raw data (dots) and spline fit (solid lines) shown. (**C**) Raw temporal expression (dot) profile and spline fit (solid line) of top three ~12h genes with the smallest p values in each of the three individuals. (**D**) Venn diagram depicting common and distinct ~12h genes for each individual, with selective common genes shown on the right. (**E**) GSEA showing enrichment score of 213 common ~12h genes on robust ~12h genes ranked by meta p values. (**F**) Heatmap and quantification of 213 common ~12h genes uncovered from all three participants. (**G**) GO analysis of all and shared ~12h genes in each individual.

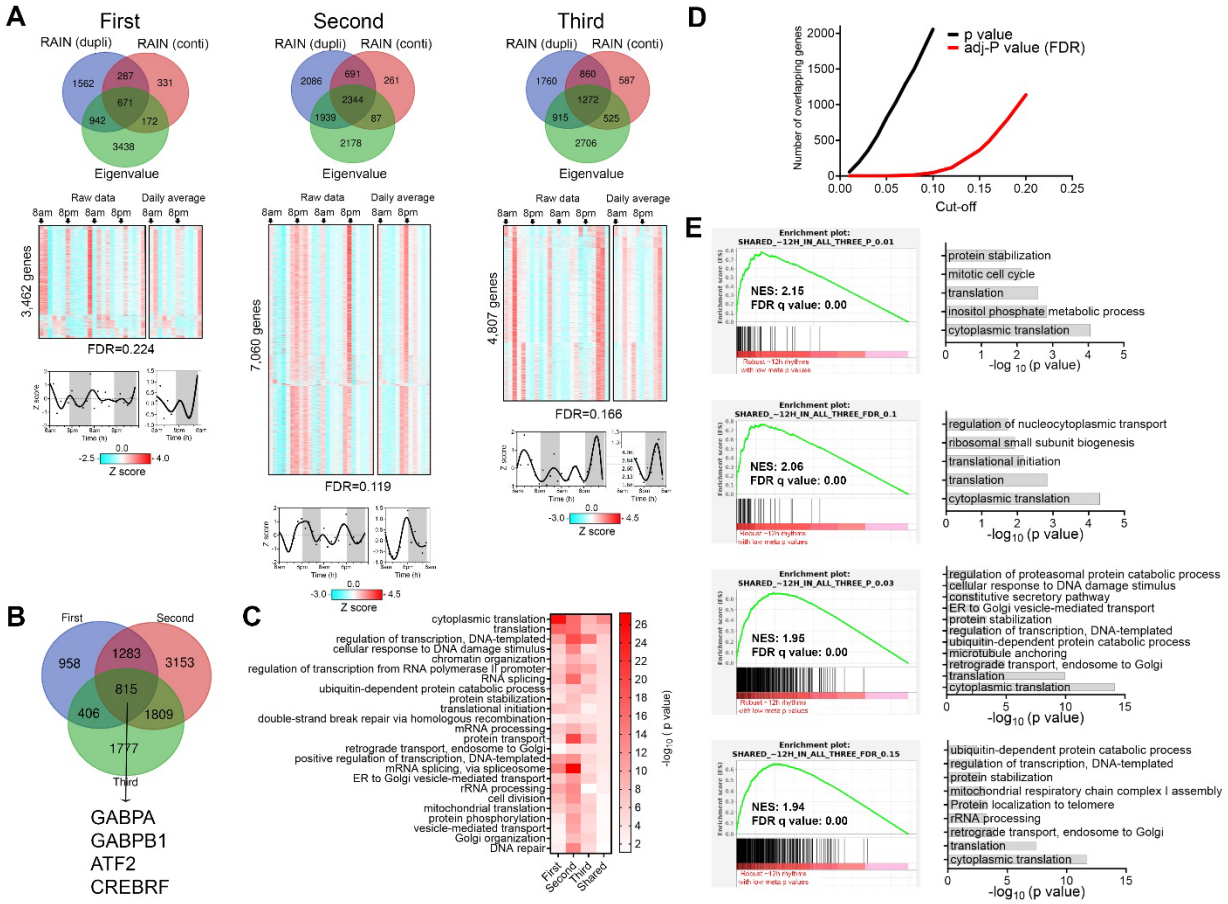

Fig. S4. RAIN analyses of temporal transcriptomes using consecutive 24 hours datasets as biological replicates. (**A**) Venn diagram comparing the ~12h programs uncovered by the three methods (top) and heatmap and quantification of ~12h genes uncovered by the RAIN dupli method in all three participants (bottom). (**B**) Venn diagram depicting common and distinct ~12h genes uncovered in each participant. (**C**) GO analysis of all and shared ~12h genes in all three participants. (**D**) Scatter plot comparing the number of overlapping ~12h genes between the three individuals against different p values or FDR cut-offs for all individuals. (**E**) GSEA showing enrichment scores for four gene sets of overlapping ~12h genes with p<0.01 (56 genes), p<0.03 (358 genes), FDR<0.1 (46 genes) and FDR<0.15 (361 genes) cut-off (left) on ~12h genes ranked by meta-p values and GO analysis of these genes (right).

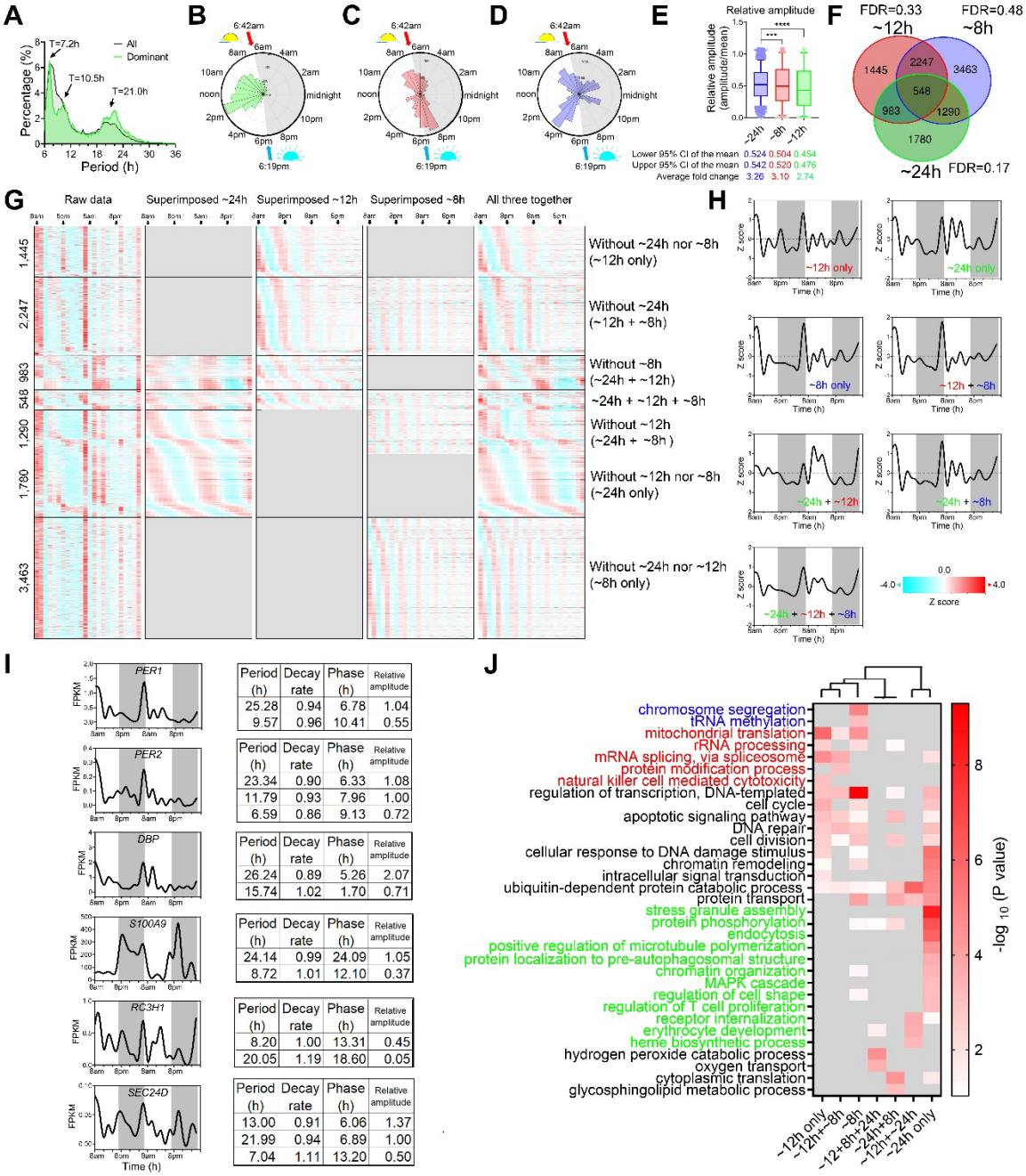

Fig. S5. Transcriptome spectrum of first human participant. (**A**) Period distribution of all and dominant oscillations. (**B-D**) Polar histogram illustrating the phase distribution of ~24h (**B**), ~12h (**C**) and ~8h (**D**) oscillations. (**E**) Relative amplitude (mean-normalized) of ~8h, ~12h and ~24h oscillations. (**F**) Venn diagram showing distinct and shared oscillations for each period. (**G, H**) Heatmap (**G**) and quantification (**H**) of decomposition of raw temporal transcriptome into harmonics cycling at ~8h, ~12h or ~24h periods. (**I**) Representative temporal expression of select genes and eigenvalue/pencil decomposition uncovering all superimposed oscillations for each gene. (**J**) GO analysis of all genes in **G**.

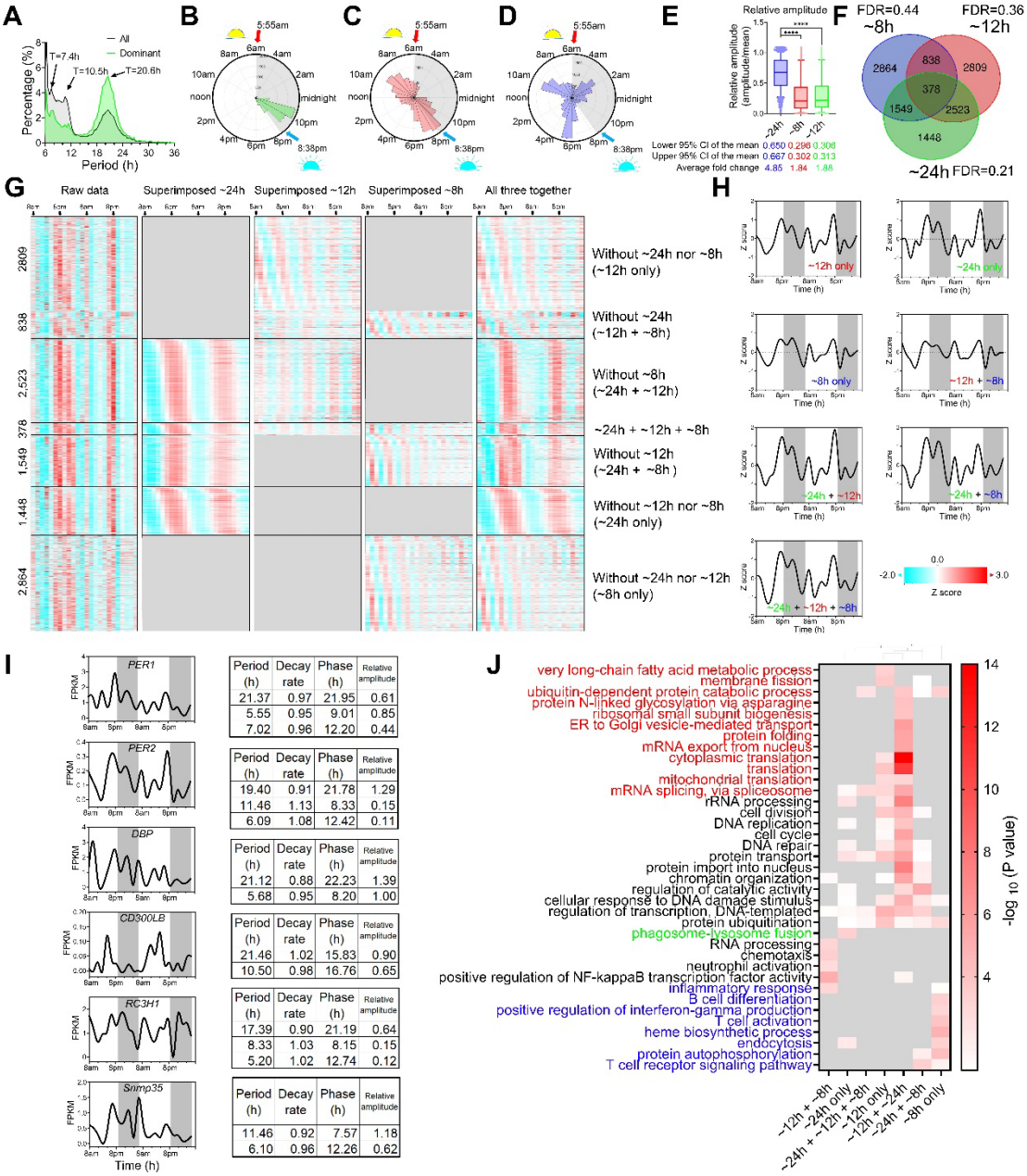

963

964 **Fig. S6. Transcriptome spectrum of the second human participant.** (**A**) Period distribution of
965 all and dominant oscillations. (**B-D**) Polar histogram illustrating the phase distribution of ~24h (**B**),
966 ~12h (**C**) and ~8h (**D**) oscillations. (**E**) Relative amplitude (mean-normalized) of ~8h, ~12h and
967 ~24h oscillations. (**F**) Venn diagram showing distinct and shared oscillations for each period. (**G,**
968 **H**) Heatmap (**G**) and quantification (**H**) of decomposition of raw temporal transcriptome into
969 harmonics cycling at ~8h, ~12h or ~24h periods. (**I**) Representative temporal expression of
970 selective genes and eigenvalue/pencil decomposition uncovering all superimposed oscillations
971 for each gene. (**J**) GO analysis of all genes in **G**.

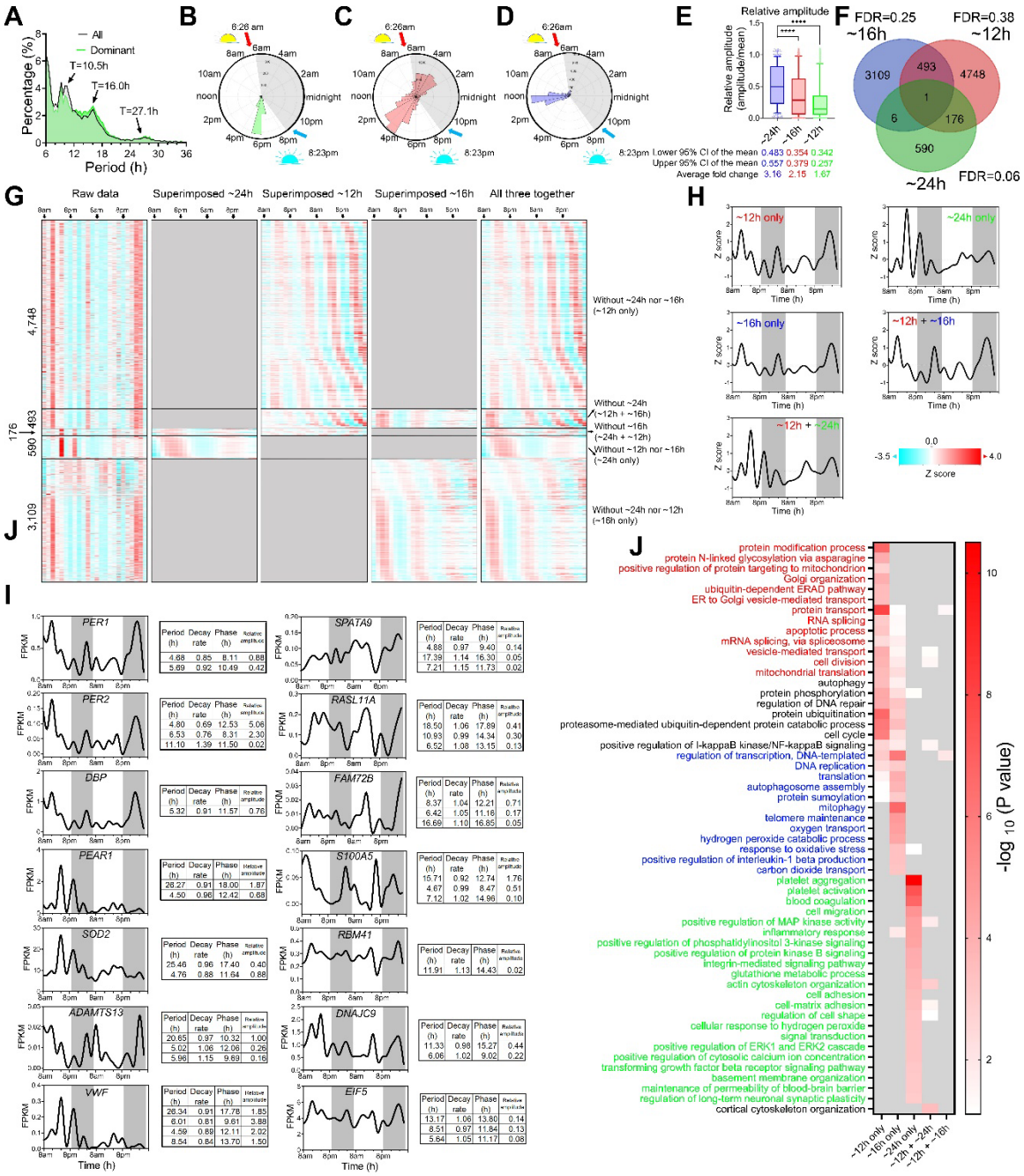

Fig. S7. Transcriptome spectrum of the third human participant. (**A**) Period distribution of all and dominant oscillations. (**B-D**) Polar histogram illustrating the phase distribution of ~24h (**B**), ~12h (**C**) and ~16h (**D**) oscillations. (**E**) Relative amplitude (mean-normalized) of ~16h, ~12h and ~24h oscillations. (**F**) Venn diagram showing distinct and shared oscillations for each period. (**G, H**) Heatmap (**G**) and quantification (**H**) of decomposition of raw temporal transcriptome into oscillations cycling at ~16h, ~12h or ~24h periods. (**I**) Representative temporal expression of selective genes and eigenvalue/pencil decomposition uncovering all superimposed oscillations for each gene. (**J**) GO analysis of all genes in **G**.

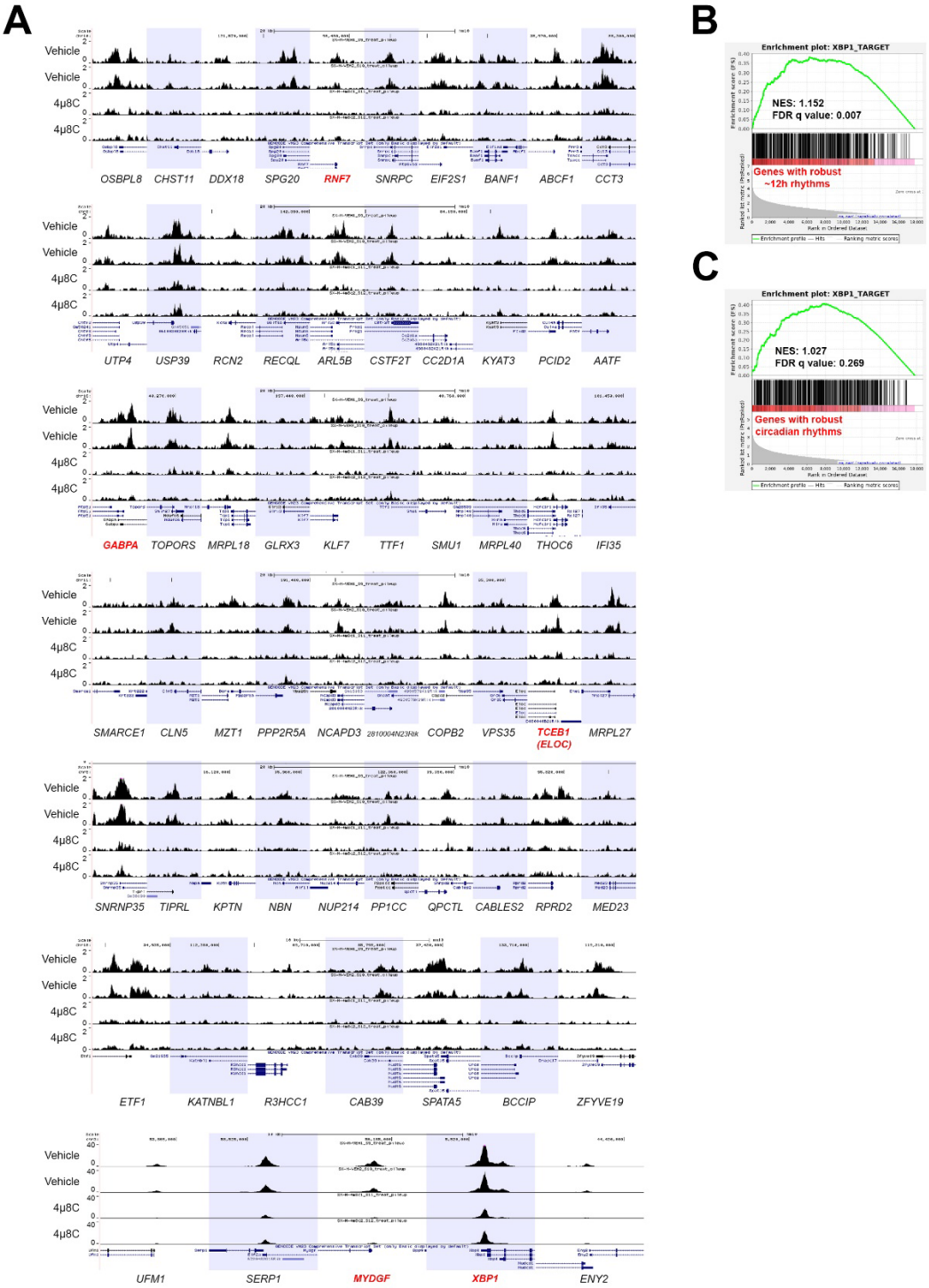

Fig. S8. XBP1 chromatin binding landscape of 12h genes in mouse Th2 cells. (**A**) UCSC genome browser view of XBP1 chromatin recruitment to the promoters of a selected set of ~12h genes in murine Th2 cells. (**B, C**) GSEA showing enrichment score of top 500 XBP1 target genes in Th2 cells (ranked by fold reduction of target gene expression with XBP1 deletion) in robust ~12h (**B**) or circadian (**C**) genes identified in humans.

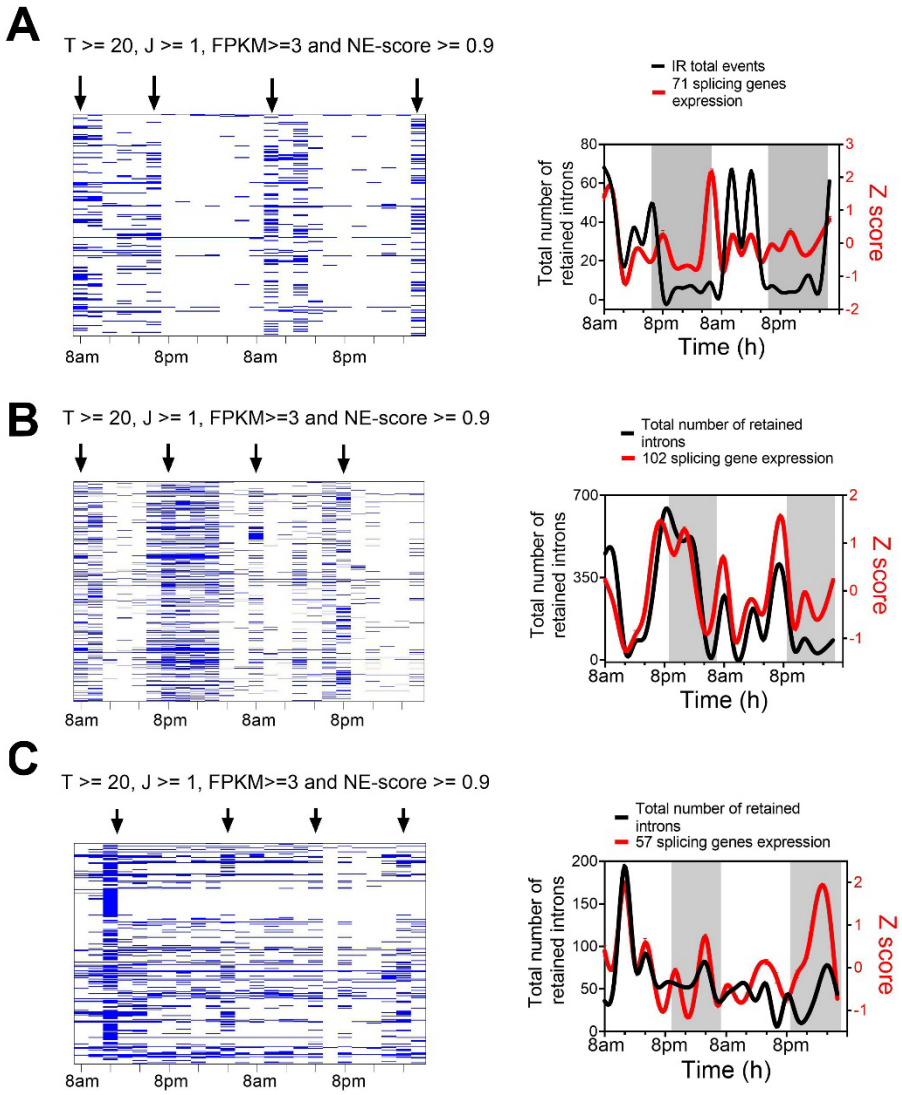

D

	Intron retention events rhythms	
	Period	p value
First	10h	0.2041
Second	12h	0.0439
Third	12h	0.0056
Meta	10-12h	2.990E-03

Fig. S9. ~12h rhythms are synchronized to global intron retention rhythms. Criterions for IR are set as T>=20, J>=1, FPKM>=3 and NE score>=0.9. (**A-C**) Heatmap (left) and quantification (right) of temporal IR events, superimposed with the Z score normalized temporal expression of ~12h splicing gene expression in the first (**A**), second (**B**) and third (**C**) participants. IR events are detected with the more stringent setting of the iRead algorithm as described in the methods section. (**D**) Statistics for IR ~12h rhythms detection by RAIN.

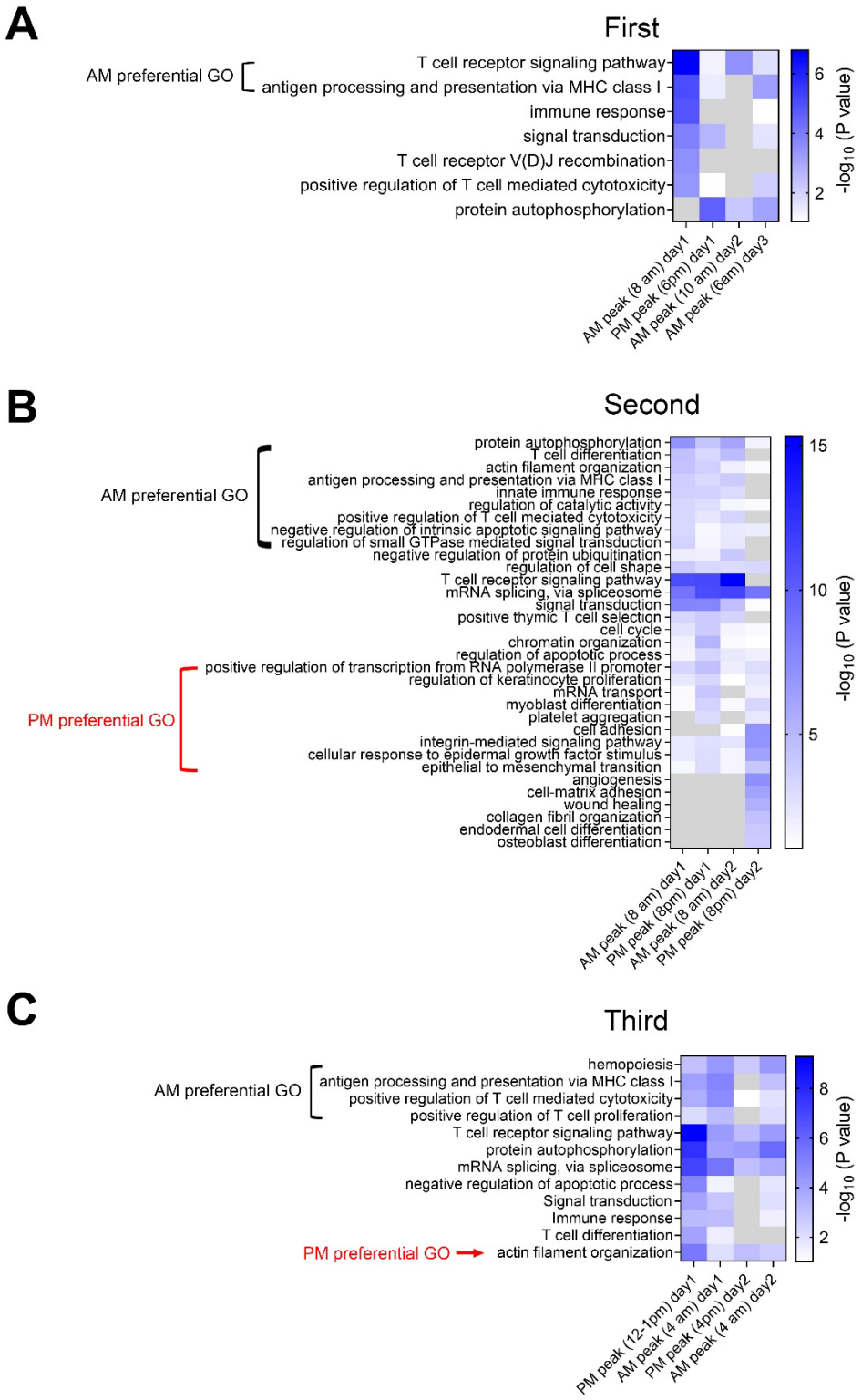

Fig. S10. Genes with intron retentions are enriched in immune genes. Intron retention events are selected with default settings T>=20, J>=1, FPKM>=2 and NE score>=0.9. GO analysis of IR genes at different peaks in the first (**A**), second (**B**) and third (**C**) participant.

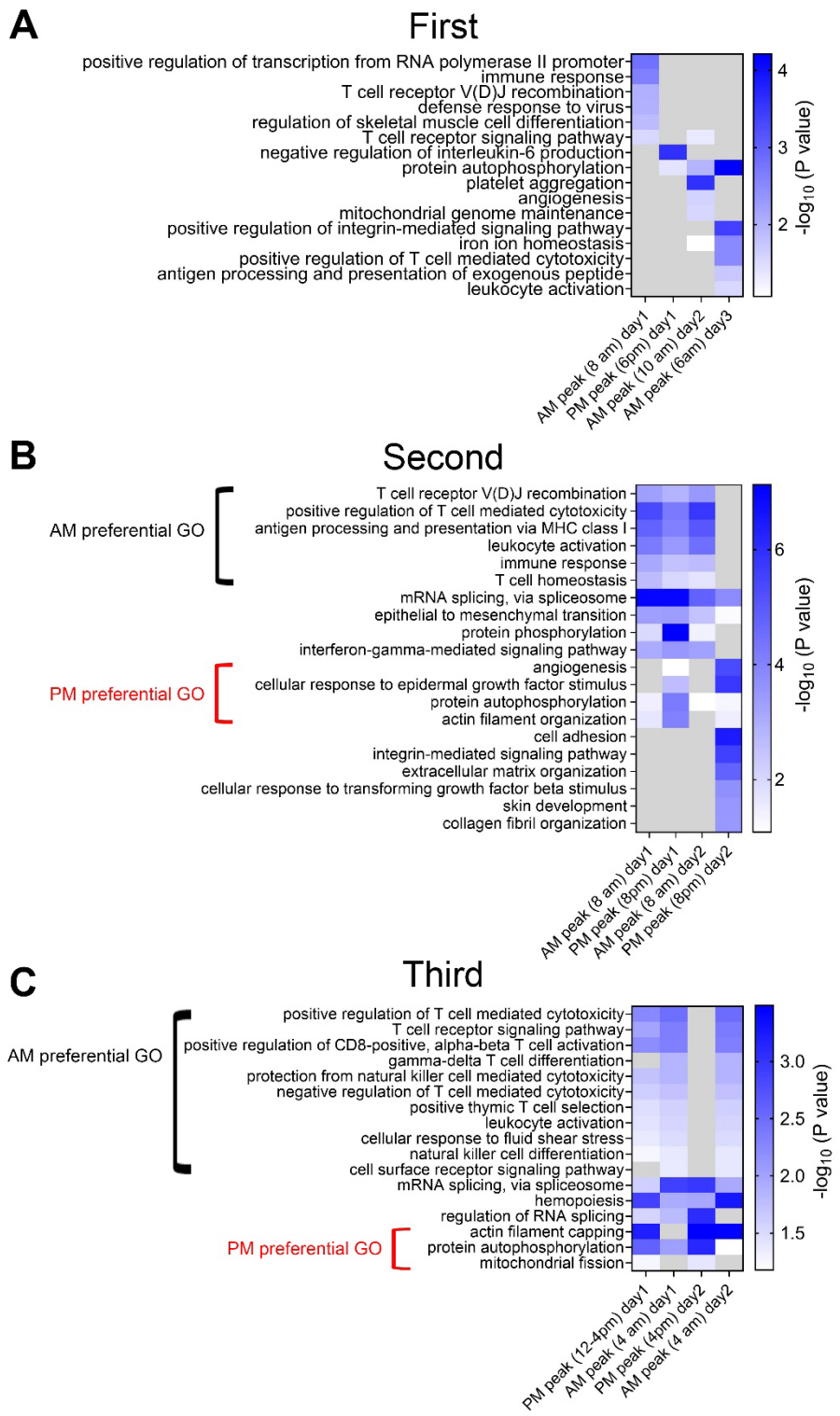

Fig. S11. Genes with intron retentions (more stringent criterion) are enriched in immune genes. Intron retention events are selected with default settings T>=20, J>=1, FPKM>=3 and NE score>=0.9. GO analysis of IR genes at different peaks in the first (**A**), second (**B**) and third (**C**) participant.

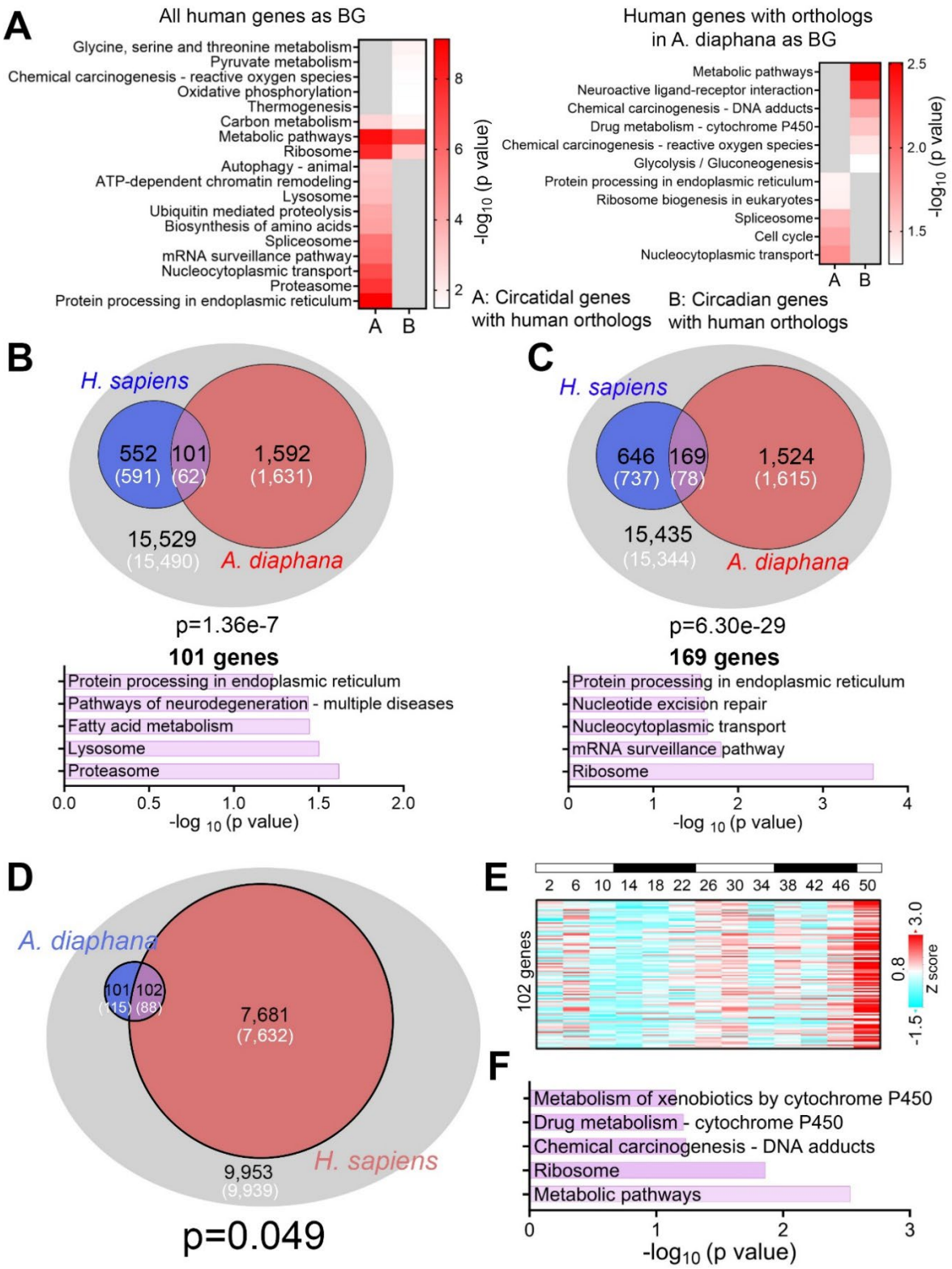

Fig. S12. Evolutionary conservation of ~12h, but not circadian gene programs between A. diaphana and human. (**A**) GO analysis of all circatidal genes in A. diaphana that have human orthologs using all human genes (left) or only those with A. diaphana orthologs (right) as

background. (**B, C**) Venn diagram comparing distinct and shared ~12h genes in human (653 12h genes with meta adj-P<0.05 in **B** and 851 ~12h genes reported in Fig. S4B in **C** and *A. diaphana* (reported in [44]). Only genes that are expressed in human white blood cells (denoted by the grey circle) are included in the analysis. Both observed and predicted number of genes (under the null hypothesis that ~12h genes are not evolutionarily conserved and thus independently detected in these two species) are further shown. P values are calculated by the Chi-square test. GO analysis showing enriched KEGG terms for the 101 and 169 common genes, respectively. (**D**) Venn diagram comparing distinct and shared circadian genes in human (meta adj-P<0.1) and *A. diaphana* (reported in [44]). Only genes that are expressed in human white blood cells (denoted by the grey circle) are included in the analysis. Both observed and predicted number of genes (under the null hypothesis that circadian genes are not evolutionarily conserved and thus independently detected in these two species) are further shown. P value of 0.049 is calculated by Chi-square test. (**E, F**) Heatmap of temporal expression (Z score normalized) of 102 circadian genes in *A. diaphana* (**E**) and GO analysis of the top enriched pathways (**F**).

Table S1. RPKM quantification of temporal expression for the human participants

Table S2. RAIN results for ~12h genes and meta-analysis of circadian genes.

Table S3. Eigenvalue/pencil results